



**TOGETHER**  
*for a sustainable future*

## OCCASION

This publication has been made available to the public on the occasion of the 50<sup>th</sup> anniversary of the United Nations Industrial Development Organisation.



**TOGETHER**  
*for a sustainable future*

## DISCLAIMER

This document has been produced without formal United Nations editing. The designations employed and the presentation of the material in this document do not imply the expression of any opinion whatsoever on the part of the Secretariat of the United Nations Industrial Development Organization (UNIDO) concerning the legal status of any country, territory, city or area or of its authorities, or concerning the delimitation of its frontiers or boundaries, or its economic system or degree of development. Designations such as “developed”, “industrialized” and “developing” are intended for statistical convenience and do not necessarily express a judgment about the stage reached by a particular country or area in the development process. Mention of firm names or commercial products does not constitute an endorsement by UNIDO.

## FAIR USE POLICY

Any part of this publication may be quoted and referenced for educational and research purposes without additional permission from UNIDO. However, those who make use of quoting and referencing this publication are requested to follow the Fair Use Policy of giving due credit to UNIDO.

## CONTACT

Please contact [publications@unido.org](mailto:publications@unido.org) for further information concerning UNIDO publications.

For more information about UNIDO, please visit us at [www.unido.org](http://www.unido.org)

09494



United Nations Industrial Development  
Organization

GROUP TRAINING IN PRODUCTION  
OF ALUMINA  
VOLUME 4

MINERALOGICAL AND TEXTURAL INVESTIGATION OF BAUXITE,  
RED MUD AND ALUMINA

ALUTERV - FKI

BUDAPEST, JULY 1979

## VOLUME 4

### MINERALOGICAL AND TEXTURAL INVESTIGATION OF BAUXITE, RED MUD AND ALUMINA

BY

Dr. P. Gadó  
Dr. M. Orbán

The opinions expressed in this paper are those of the author(s) and do not necessarily reflect the views of the secretariat of UNIDO. This document has been reproduced without formal editing.

Printed in  
ALUTERV-FKI's Printing Shop  
in 1979/1055

## CONTENTS

FIGURES	4-III
1. INTRODUCTION	4-1
2. METHODS OF BAUXITE INVESTIGATIONS	4-2
Textural Investigations	4-2
Electron Microprobe Analysis (EPMA)	4-8
Scanning Electron Microscopy (SEM)	4-19
Transmission Electron Microscopy (TEM)	4-25
Mineralogic Investigations	4-27
Thermal Methods	4-39
Infrared (IR) Absorption Spectrometry	4-48
Partial Dissolution Tests	4-60
Mossbauer Spectrometry	4-52
Optical Methods	4-63
Other Complementary Methods	4-65
Quantitative Phase Analysis of Bauxite	4-66
3. MINERALOGICAL INVESTIGATION OF RED MUD	4-87
X-ray Diffractometry	4-91
Thermal Methods	4-95
IR Spectrometry	4-98
Quantitative Phase Analysis of Red Muds	4-101
4. MINERALOGICAL INVESTIGATION OF ALUMINA	4-102
Optical Methods	4-102
X-ray Diffraction Methods	4-102
REFERENCES	4-105

## FIGURES

- Fig. 4.1 Quantitative evaluation of a microscope image using an auxiliary square grid 4-4
- Fig. 4.2 A schematic representation of the interaction of an electron beam with a solid of moderate or low atomic number 4-7
- Fig. 4.3 EPMA study of a bauxite specimen 4-11
- Fig. 4.4 A typical spherical particle in a bauxite sample investigated by EPMA technique 4-12
- Fig. 4.5 Matching reflected electron-/A/, Y L-alpha /B/ and P K-alpha /C/ X-ray intensities permit the assumption that a xenotime grain was found 4-14
- Fig. 4.6 Measurement of Zn distribution along a line in a bauxite sample 4-16
- Fig. 4.7-A Si K-alpha and Fe-K-alpha X-ray line scans, respectively. The two intensities change simultaneously 4-17
- Fig. 4.7-B Al and Fe concentrations seem to be complementary according to the line scans made with the corresponding K-alpha X-rays 4-18
- Fig. 4.8 Images of some meshes used for testing SEM apparatus 4-21
- Fig. 4.9 SEM /secondary electron/ image of ankerite crystals 4-21
- Fig. 4.10 Toothlike crystallites on the flat surface of an ankerite crystal 4-22

Fig. 4.11-A	Typical view of the video display of an ED X-ray analyser. The labels yield good many information	4-24
Fig. 4.11-B	Particle size histogram of a bauxite sample based on TEM measurements	4-26
Fig. 4.12	Electronmicroscopic /TEM/ photograph of a bauxite sample	4-26
Fig. 4.13	Diffraction from a powder specimen	4-31
Fig. 4.14	Block diagram of a typical X-ray diffractometer set-up	4-31
Fig. 4.15	Geometry of the goniometer	4-32
Fig. 4.16	Diffraction pattern of a mixture of ZnO and Al <sub>2</sub> O <sub>3</sub>	4-32
Fig. 4.17	Tabulated diffraction data from ZnO plus $\alpha$ -Al <sub>2</sub> O <sub>3</sub> /measured from the diffractogram of Fig. 4.16/	4-35
Fig. 4.18	The PDF card of alpha-Al <sub>2</sub> O <sub>3</sub>	4-36
Fig. 4.19	Simultaneous DTA, DTG of boehmites	4-45
Fig. 4.20	Simultaneous TG, DTA of diaspore	4-47
Fig. 4.21	"Derivatogram" of a goethitic bauxite sample	4-47
Fig. 4.22	Absorption IR-spectra of the main bauxite-forming minerals	4-51
Fig. 4.23	Infrared spectra of haitian bauxite	4-53
Fig. 4.24	Infrared spectra of low-grade jamaican bauxite	4-54

- Fig. 4.25 Definition of IR extinction, determination of the baseline in an IR absorption spectrum 4-55
- Fig. 4.26 Relationship between "reactive  $\text{SiO}_2$ " & and the intensity ratio  $\text{kaol} \frac{910 \text{ cm}^{-1}}{965 \text{ cm}^{-1}}$  4-55
- Fig. 4.27 Infrared spectra of bauxites with range of total  $\text{SiO}_2$  content 4-58
- Fig. 4.28 Infrared absorption spectra of aluminogothites in the  $700\text{-}1200 \text{ cm}^{-1}$  wave number range 4-58
- Fig. 4.29 The shift of wave number for the goethite band near  $900 \text{ cm}^{-1}$  vs. aluminium percentage 4-59
- Fig. 4.30 The  $\text{Al}_2\text{O}_3$  /boehmite/ yield of various bauxites as the function of the wave number corresponding to the boehmite band 4-59
- Fig. 4.31 Computer processed diffractogram of a bauxite sample 4-73
- Fig. 4.32 The  $d_{111}$  lattice parameter of goethite as a function of Fe/Al substitution 4-74
- Fig. 4.33 The final of results is printed, a sample of which can be seen on Fig. 4.33 4-76
- Fig. 4.34 DTG and TG curves of a mixed bauxite and of red muds obtained three different digestion temperatures 4-78
- Fig. 4.35 The relative breadth of the 020 X-ray reflection from three bauxites. The original bauxites and some fractions were measured as marked on the horizontal axis 4-85

- Fig. 4.36 X-ray diffraction traces of goethite in bauxite /A-D/ and muds /E-J/ showing variations in aluminium substitution 4-86
- Fig. 4.37 Scanning micrograms of a red mud /A/ and two of its significant components: cancrinite /B/ and  $\text{CO}_3$  sodalite /C/ 4-88
- Fig. 4.38 The derivatogram of sodalite and carbonate sodalite, important components of red mud 4-97
- Fig. 4.39 Calibration curve for the determination of undissolved boehmite in red mud by the  $3100 \text{ cm}^{-1}$  infrared band 4-97
- Fig. 4.40 Calibration curves for the determination of cancrinite in red mud 4-100



## 1. INTRODUCTION

Mineralogical tools and methods are extensively used in the alumina industry. This fact can easily be understood referring to the experiences of the technologists that the commercial value of bauxites, the expected behaviour of intermediate products in the Bayer process like red muds and other materials related to it, as well as the quality of the alumina prepared in a definite plant can be only assessed if data characterizing the morphology (structure, texture and porosity), qualitative and quantitative mineral composition and the quantitative elemental (chemical) analysis are made available.

The problems of bulk chemical analysis are tackled elsewhere in this work. Morphologic studies concern the shapes and dimensions of particles, grains which constitute the materials investigated as well as similar characteristics of the agglomerates formed by the primary units. Chemical composition of the various morphologic units is a closely related information and the microdistribution of elements will be discussed in this context. From the point of view of mineralogy bauxite, red mud and alumina are composite materials. These multicomponent powder mixtures can be analysed for the constituent mineral phases which possess already uniquely defined crystal structures. Beyond the methods used for identification of the phases present (qualitative analysis), the methods of determining their proportions (quantitative analysis) will be described, too.

This survey will concern both the classical and up-to-date instrumental techniques most frequently used in mineralogic evaluation of the three main groups of materials occurring in the Bayer alumina production. Emphasis will be placed on the quantitative procedures based on advanced physico-chemical principles. It can not be the aim of this paper to outline the full background of all disciplines ap-

plied in the field of the mineralogical analysis, however, we will introduce each method by simple reasoning indicating the essential and specific informations gained by the particular techniques and describing the necessary equipment, too. Among the diverse methods of mineralogical materials research X-ray diffraction (XRD), infrared absorption spectrometry (IR) and thermal analysis (TA) have preferred role and are being exploited in all sectors of alumina production. The common features of these research procedures will be described when handled first in the following text and only the specific differences underlined for the further applications.

## 2. METHODS OF BAUXITE INVESTIGATIONS

### TEXTURAL INVESTIGATIONS

The size, shape and mutual arrangement of the mineral grains and various particles forming any rock is referred to as its texture. We mean by textural investigations all those studies which yield information and accurate data about the distribution of chemical elements and mineral phases as well as about the size, form and distribution of pores, flaws, etc. within the ore. Detailed classification of the 14 different elements of texture and of the 19 simple types of textures found in karstic bauxites, together with the relative frequencies of these is given in the recently published book of Bårdossy (1978). When determining the commercial value of a bauxite the textural features characteristic for the whole deposit must be emphasized and the rarely occurring ones must be suppressed, however interesting or esthetically appealing they might be. Textural investigations can and must be carried out with different special resolutions ranging from the mm dimensions down to the  $\mu$ m sized details.

### Macroscopic Studies

Macroscopic characteristics of the texture can be revealed by the naked eye on a broken surface of the sample. In this way one could distinguish between the rather homogeneous basic material of the bauxite and the inclusions occurring in it, like splinters of other rocks (inclusive bauxite), veins, pizoides or any other particles exceeding in size 0.1 mm.

Observing the colour and characteristic crystalline shape of some particles ideas can be put forward regarding the presence and distribution of iron minerals, clays, etc. In order to establish the textural type of a given bauxite deposit statistically significant amount of data must be collected and if the elements of texture are not very finely dispersed macroscopic methods can be preferable since a surface of say 50 x 50 mm<sup>2</sup> area can be investigated in one step.

### Microscopic Studies

For the purposes of textural studies by means of a light microscope microsections have to be prepared. These are finely polished almost plan-parallel slices of some 0.1 mm thickness. Fairly hard bulk material is necessary that one should be able to cut rather thin slices, glue them on a glass substrate and then polish to the required final thickness.

Depending on the size of the particles to be discerned microphotographs are taken with magnifications between 2x and 1000x. In bauxite microsections the parts of the rock rich in iron appear generally dark while other minerals are more or less transparent. Carefully evaluating the micrographs a quantitative determination can be attained regarding the dispersion of the bauxite constituents provided the dimensions of the details are in the  $\mu$ m range or above. (Fig.4.1)

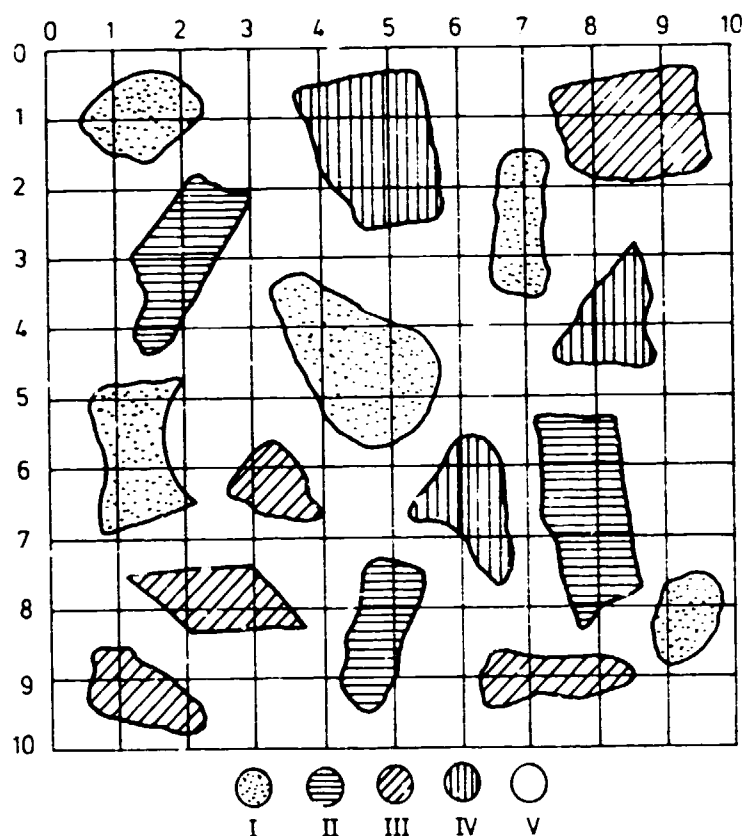


Fig. 4.1  
 QUANTITATIVE EVALUATION OF A MICROSCOPE IMAGE  
 USING AN AUXILIARY SQUARE GRID

The largest linear extension of the individual particles is summed both in horizontal and vertical directions for the phases marked differently (I,II,III,IV) and for the matrix (V). In the depicted image the percentages of the five constituent are:

I.	9.9	%
II.	7.9	
III.	6.0	
IV.	5.8	
V.	70.2	(matrix)

(from Strókai and al.: Ásványtani praktikum II.  
 Tankönyvkiadó, Budapest, 1970. p.108-109.)

Similar information can be gained from X-ray microradiographic studies. Here the microsections are exposed to an X-ray beam uniform in intensity over its cross-section and of adequate wavelength. The shadow image is then recorded on a photographic plate held in contact with the microsection. Positive prints of this plate can be prepared in high magnifications (10-20x). Since the absorption of X-rays increases in function with atomic number, light elements (Al, Si, etc.) are more transparent than minerals containing heavier ones (Ti, Fe, Ca, etc.). Good photographic technique permits high resolution both in a geometrical sense (about 1  $\mu$ m) and in chemical constitution (third neighbours in the periodic table yield considerable difference in transmission when appropriate wavelength is used).

Although microsection studies give valuable contributions to texture studies, since the advent of powerful electronbeam methods the latter are more frequently applied partly because they require less tedious preparation of the samples.

#### Electron beam studies

Part of the challenge in many technological problems arises from the way in which some small, microscopic particles control the macroscopic development of the whole process. In mineralogy often complex shapes have to be studied to resolutions of the order of 1  $\mu$ m with a large depth of focus. In this range electron optical instruments are playing a highly significant role. Here we will deal with the applications of three major methods: X-ray microanalysis, scanning electron microscopy and transmission electron microscopy.

Common feature of these investigations is, that they are based on the interactions of electrons with materials. The electrons are produced most commonly by thermionic emission from a heated tungsten filament (cathode). The emerging electrons are accelerated by a high voltage connected between the

hot wire a metal aperture (anode). The electrons traveling with high speed in an evacuated column will be restricted by means of an electrooptical system of appropriate lenses to a narrow and intensive beam impinging upon the sample. Fig.4.2 illustrates the effects caused by the electron-material interaction. We intend to deal only with a few of these interactions, namely: 1) the production of X-rays exploited for microanalysis (first of all in the electron probe microanalysers (EPMA), 2) the appearance of secondary electron and that of backscattered ones is the basis of scanning electron microscopy (SEM) and 3) the absorption as well as the phase shift of the transmitted electrons (the wave aspect of which is emphasized in this application) give rise to the possibility of image formation in the transmission electron microscopy (TEM). Although the above three electron beam methods will be described separately, very useful combinations of these have been developed, too.

It seems to be reasonable to explain the scanning principle in this introductory phase, because it had been essential from the very beginnings in EPMA and SEM instruments, however, recently it became extensively used also in TEM.

In scanning devices the electron beam is not stationary but the extremely small spot of electron illumination (diameter about  $1 \mu\text{m}$ ) is swept by a varying electrostatic field in a regular pattern across a small area of the sample (e.g. a few  $\text{mm}^2$ ). The signal due to a selected effect of the electrons is then appropriately processed in an electronic channel and displayed on a cathode ray tube (CRT). The cathod ray in the CRT is moved in synchronism with the primary electron beam bombarding the sample. Since the brilliance in each spot of the CRT is made proportional to the electron-induced effect detected from the corresponding point of the specimen, a one-to-one mapping of the scanned surface occurs on the CRT. Control of the scanning pattern permits the observation and

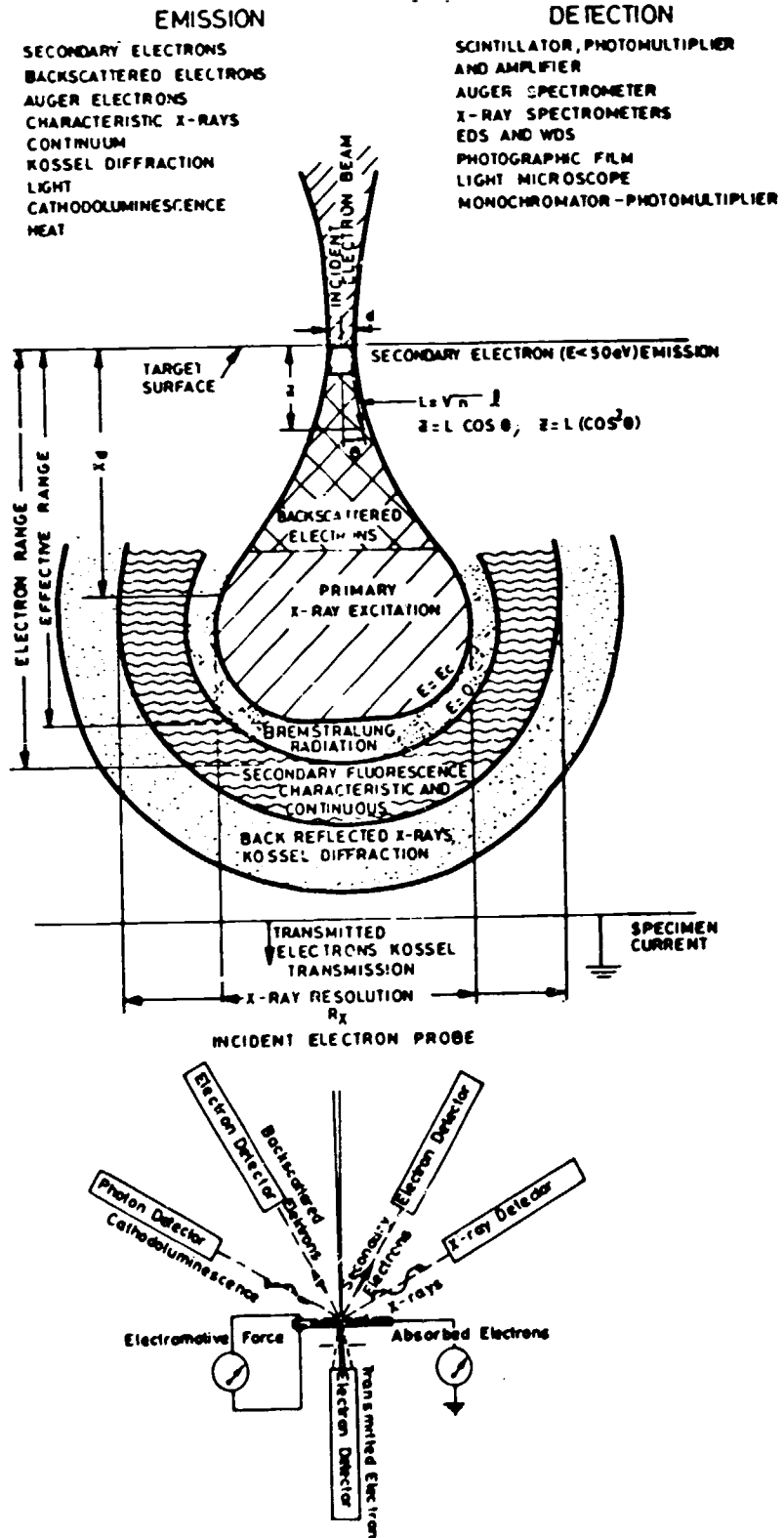


Fig. 4.2

A SCHEMATIC REPRESENTATION OF THE INTERACTION  
 OF AN ELECTRON BEAM WITH A SOLID OF MODERATE  
 OR LOW ATOMIC NUMBER

photographic or chart recording of different regions of the specimen: spot-by-spot measurement, line scan or surface scan.

#### ELECTRON MICROPROBE ANALYSIS (EPMA)

Electron microprobe analysis reveals the textural characteristics of bauxite samples in a sense that the special distribution of the constituting chemical elements can be detected on a micro-scale.

The samples for EPMA investigation must have a polished surface of optical quality. This can be achieved fairly simply when solid lumps of the mineral are available. The largest dimension of the piece mounted onto the sample holder should generally not exceed 15 mm. However, usually a thin slice is cut from the mineral and then ground and polished by abrasive materials. Since some grains of the abrasive inevitably adhere to the sample the former should not contain any elements to be analysed. Thus corundum abrasive must be avoided when preparing samples for the study of distribution of aluminium minerals, however diamond paste is an appropriate polishing material in most cases. Electrons have a very low penetration depth thus rather thin sections are sufficient. The specimens must be electrically conductive in order to escape from effects connected with static charging by the beam. Insulating materials can be rendered conductive applying a thin conductive layer on the surface (evaporated C,Cu,Ag,Au, etc.).

The main parts of a microanalyser are:

- the electron optical column with evacuation system
- the spectrometers and divers detectors
- electronic operation and control system including power supplies
- computer controlled measuring and display units.



The column is evacuated by rotary and diffusion pumps to  $10^{-5}$  -  $10^{-6}$  Torr pressure. Safety circuits protect the instrument against working in insufficient vacuum. The electron optical system comprises an electron gun, a condenser and an electromagnetic stigmator lens to correct for astigmatism. The electron probe at the analysing position can be observed by means of its cathodoluminescent image through an optical microscope provided also with illuminator for visual observation and microphotography. The magnification goes typically up to 400x, the resolving power should be better than  $1 \mu\text{m}$ . Accelerating voltage and beam current being fully stabilized prolonged measurements can be carried out effectively. The probe diameter can be reduced so far that the volume analysed by X-ray spectrometry can be restricted to about  $2-5 \mu\text{m}^3$ .

Up-to date microanalysers incorporate several vacuum spectrometers so that three or four elements can be analysed simultaneously. Each spectrometer is equipped with several analyser crystals selected according to the chemical elements to be measured and detectors: proportional or scintillation counters. The spectrometer may scan a definite range of X-ray wavelength or be set to a particular value of wavelength. In the first case one can identify the elements present in a microvolume, in the second a special distribution of an element can be surveyed.

The spectrometers detect any elements between  $^5\text{B}$  and  $^{92}\text{U}$ .

It would be too lengthy to describe in all details the electronic circuits needed in a microanalyser to ensure reliable good quality measurements. We must confine the discussion here to the statement that a signal is produced which yields quantitative information about the elements present in the irradiated volume. Usually a variety of devices are provided in order to display the produced signal(s):

1. the counts representing X-ray intensity can be read from scalers, digitally printed or recorded on punched tape;
2. strip chart recorders permit analogue representation;
3. cathode ray tubes (CRT) are available to display on their screens the signals coming from each spectrometer;
4. recently the operation of microanalysers is controlled by microcomputers or microprocessors which also collect the measured data and if required process or store them. Data storage occurs usually with magnetic floppy discs.

EPMA has been applied extensively in the textural investigations on bauxites. This is reflected in many papers (Bárdossy and Panthó 1971; Bárdossy and Panthó 1973; Bárdossy, Vassel and Árkossy 1975; etc.). Below a few selected examples will be mentioned which may illustrate the kind of information electron beam microanalysis yields about different textural features of bauxite samples.

Fig.4.3-A shows the reflected electron image of a bauxite sample. It is trivial that in this ore grains of one mineral with 10-20  $\mu\text{m}$  linear dimensions (pseudomorphous substance) are separated by a network of veins. Element distribution pictures further reveal that the grains consist mainly of ferrous material (Fig.4.3-B) while the aluminium content is restricted to the fissures (Fig.4.3-C). The mineral form of the aluminous and ironous material must be determined, of course, by some other structure sensitive methods.

Spherical features (ooliths, pozooids, spastoids) form another important group of texture elements in bauxites. The reflected electron image of Fig.4.4-A shows clearly a spherical particle of 0.4 mm diameter surrounded by a matrix. Also the layered structure of this particle is clear. Several spherical



A.



Fe

B.



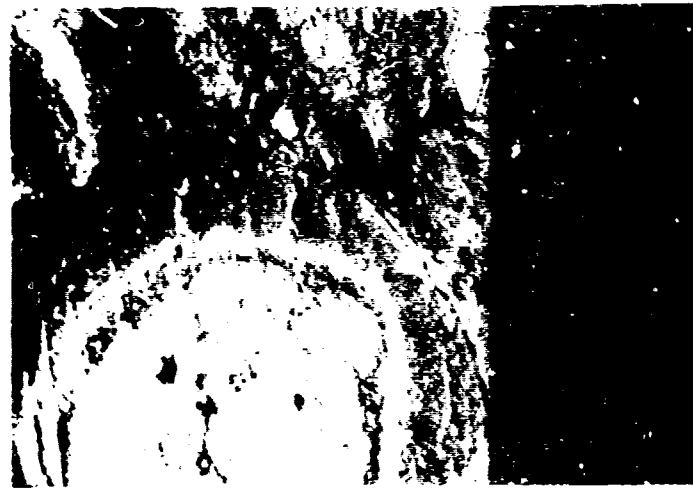
C.

Al

10  $\mu$ m

Fig. 43

EPMA STUDY OF A BAUXITE SPECIMEN



A.



B.



C.

10  $\mu\text{m}$

Fig. 4.4

A TYPICAL SPHERICAL PARTICLE IN A  
BAUXITE SAMPLE INVESTIGATED BY EPMA TECHNIQUE

shells can be distinguished with varying iron concentrations (Fig. 4.4-B). The number of such shells is usually 4-6 in the ooliths. Fig. 4.4-C shows that the matrix around the oolith is rather rich in finely dispersed Mg. what may be interpreted as due to dolomite.

It is essential that in the pictures taken with different signals (reflected electrons, characteristic X-rays, etc.) the same area of the specimen should be photographed with constant magnification in order that the correlations among the different pictures could be established.

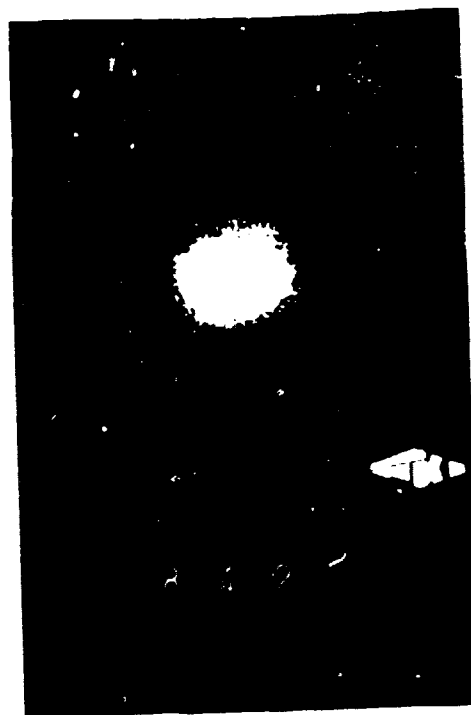
The significance of this is demonstrated by Fig. 4.5-A, B, C taken during the search for trace elements and the corresponding trace minerals in bauxites. The coincidence of Y L-alpha X-ray intensity (B. image) with high P K-alpha intensity (C. image) at the exact position of a particle of about 1  $\mu$ m size gives support for the view that here is found a grain of xenotime. Such trace minerals contain elements occurring in concentrations less than 0.5 %. The trace elements can be homogeneously distributed, or can be present in well defined textural units (ooliths, crusts, etc.) or in separate trace minerals. The latter case is proved for the bauxite giving rise to the images of Fig. 4.5. Most important trace minerals found in bauxites by EPMA investigations are chalcopyrite, sphalerite, galena, barite, monazite, zircon, members of the bastnäs site group. The study of trace minerals' and trace elements' distributions can be used effectively as a key in the research of source rocks of bauxite deposits.

In order to identify minerals in bauxite textural studies by means of EPMA the quantitative determination of concentrations is necessary.

4-14



A.  
10  $\mu$ m



B.



C.

Fig. 4.5

MATCHING REFLECTED ELECTRON-/A/, Y L-ALPHA /B/  
AND P K-ALPHA /C/ X-RAY INTENSITIES PERMIT THE  
ASSUMPTION THAT A XENOTIME GRAIN WAS FOUND

Fig.4.6 shows the line scan of Zn K-alpha X-ray intensity (B) along a line displayed in the reflected electron image (A). Deflection from the horizontal straight line in this CRT representation is proportional to the Zn concentration. Comparison with a standard sample permits the determination of Zn concentration in the grain near to the centre of the image.

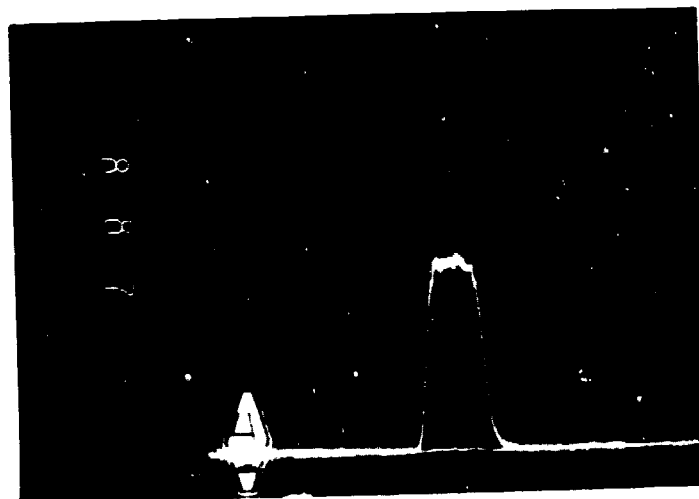
Comparative line scans prepared with well selected characteristic X-ray intensities simultaneously in several channels of the recording electronics makes possible to detect coincidence or anti-coincidence or lack of correlation between certain elements in minerals. In Fig.4.7-A the Si K-alpha and Fe K-alpha X-ray intensities change in the same direction along the sample, thus Si and Fe seems to be combined in the units of texture.

On the other hand, the line scans of 4.7-B demonstrate that Al and Fe are anti-coincident in the same sample. Consequently these elements are included in different textural elements (e.g. one of them in the matrix and the other in some particles).

The preceding figures might have illustrated the use of CRT display for two dimensional imaging of elemental distributions, the use of scanning and recording of X-ray intensities along a line for locating and measuring of high intensity in definite sites and the scalers provided within the electronic units can be applied for very exact analysis in selected points or small areas. Using appropriate reference specimens it is possible to identify by electron probe chemical analysis the mineral species which constitute the the characteristic texture features.



A.

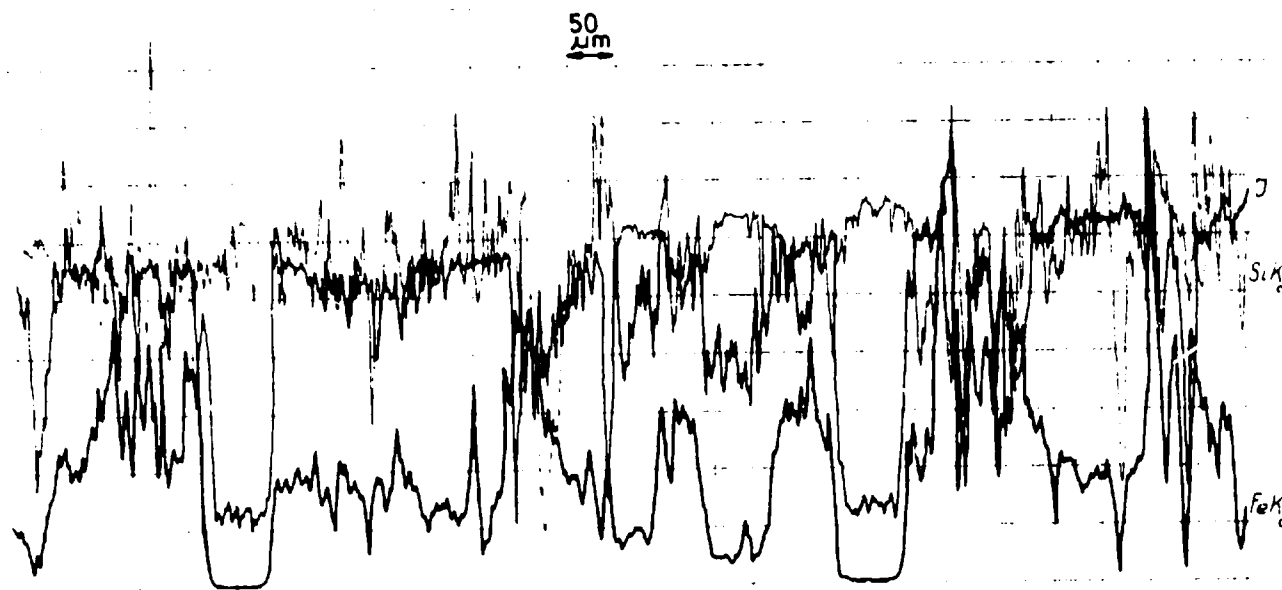


B.

1 μm

Fig. 4.6  
MEASUREMENT OF Zn DISTRIBUTION ALONG A LINE IN A  
BAUXITE SAMPLE





4-17

Fig. 4.7-A  
Si K-ALPHA AND Fe-K-ALPHA X-RAY LINE SCANS, RESPECTIVELY.  
THE TWO INTENSITIES CHANGE SIMULTANEOUSLY

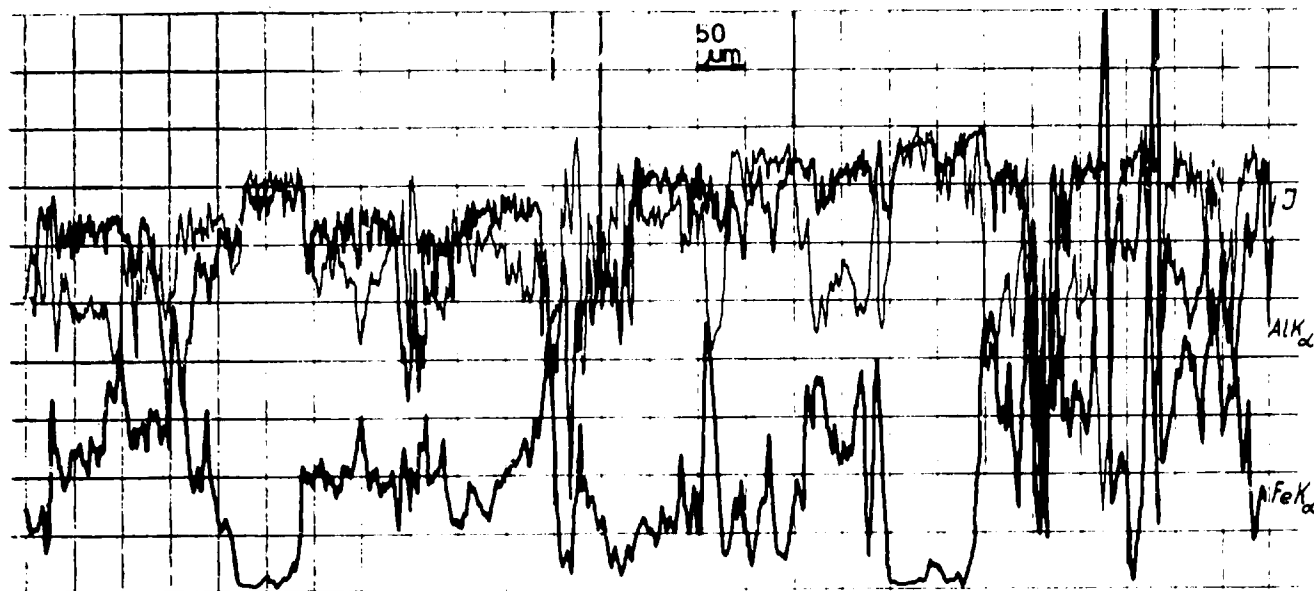


Fig. 4.7-B

Al AND Fe CONCENTRATIONS SEEM TO BE COMPLEMENTARY ACCORDING TO THE LINE SCANS MADE WITH THE CORRESPONDING K-ALPHA X-RAYS

## SCANNING ELECTRON MICROSCOPY (SEM)

Scanning electron microscopes are used in mineralogic studies usually with six different detectors producing the following images:

Image	Information
1. Secondary electron	Geometrical relief (morphology)
2. Backscattered electron	Average atomic number Geometrical relief
3. Absorbed electron	Average atomic number
4. Transmitted electron	Internal structure
5. Cathodoluminescence	Distribution and concentration of fluorescent materials
6. X-ray	Distribution and concentration of chemical elements in the Na-U range

From the "Information" column of this table it can be seen that not all images give unique data, therefore the use of secondary electron images + backscattered electron images + energy dispersive X-ray analysis seems to be a basic requirement in SEM studies and the other signals can be used additionally as the particular problem renders it indispensable. For bauxites the above combination is normally sufficient.

Scanning electron microscopes yield magnifications between about 30x and 150.000x and the resolving power is approximately 6-7 nm. By this virtue they partly bridge the gap between the optimal area of light microscopes and that of transmission electron-microscopes, and partly provide characteristic advantages as compared to these two reveals.

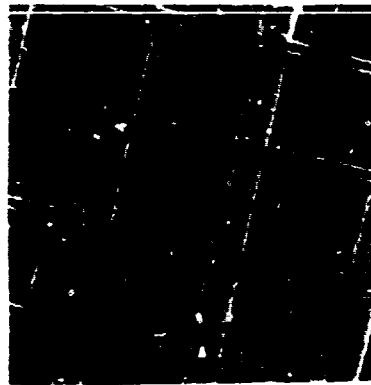
One merit that mineralogists appreciate highly is that SEM-s possess an extremely large depth of focus. On the test image of Fig.4.8 three meshes are shown with low magnification (280).

The periodicity of the square grid nearest to the observer is about 100  $\mu\text{m}$  and the distance from the top mesh to the bottom one is approximately 90  $\mu\text{m}$ . Nevertheless, all three meshes can be clearly observed. The depth of focus becomes, of course, smaller with an increasing magnification, however, it remains still very good up to about 10.000x. This means that the morphology of crystals and individual mineral particles can be studied excellently by means of SEM photographs, because the whole form, cavities, pores, etc. can be seen equally focused on the same image.

Secondary electron images give a three dimensional impression similar to that accustomed to in the macroscopic world through our daily experiences. This can be well illustrated e.g. by Fig.4.9. This can be enhanced by taking stereo pairs under slightly different angles of exposures. Since all SEM photographs are made using the signals of sensors aligned under a skew angle to the specimen surface the visual interpretation of forms and dimensions can be easily misleading so quantitative conclusions need a careful evaluation of stereo pairs. This can be aided by a computer program and the true three dimensional shape and size can be restored exactly in this way.

Another advantage of SEM is the ease of sample preparation. Bulky specimens can be observed directly without the necessity of slicing and replication, thus rough "as broken" surfaces can be studied directly and the morphology is not altered by the preparation procedure.

4-21



0.1 mm

Fig. 4.8  
IMAGES OF SOME MESHES USED FOR TESTING  
SEM APPARATUS



Fig. 4.9  
SEM /SECONDARY ELECTRON/ IMAGE OF ANKERIT CRYSTALS

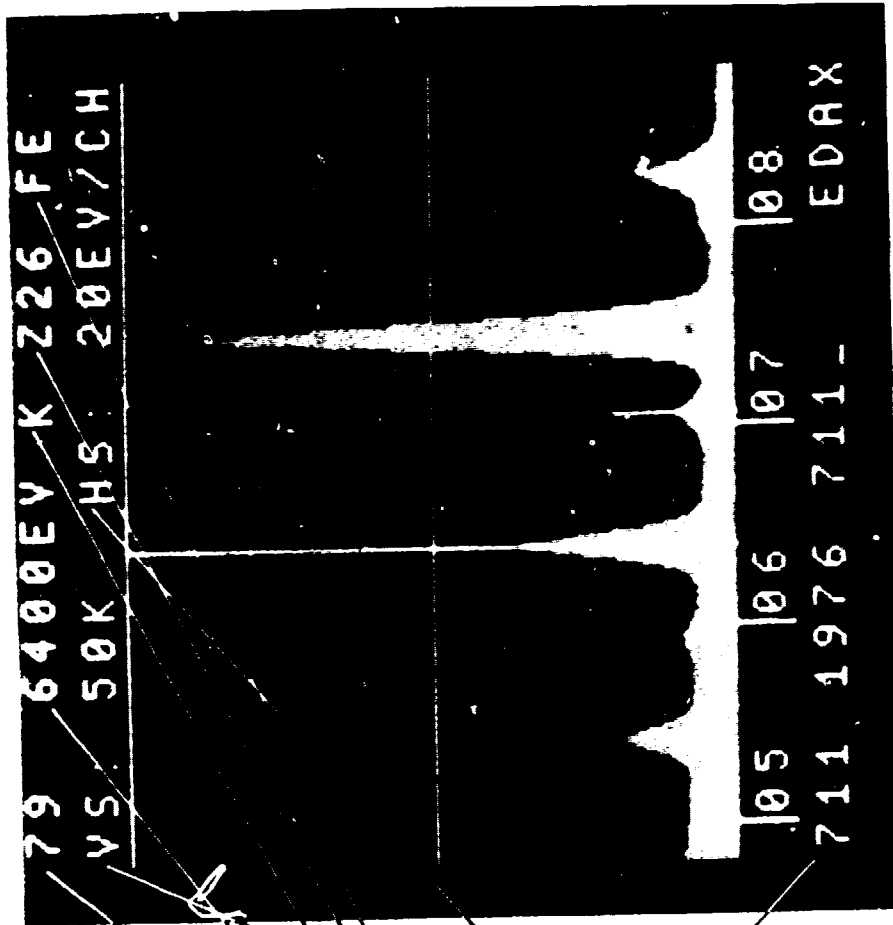
These properties render the scanning electron microscope an outstanding tool for the investigation of the texture of bauxites. Bárdossy, Csanády and Csordás publishing SEM photographs for 46 karstic, 18 lateritic and a tichvin type bauxite deposits characterize each sample by means of: the size and shape of individual crystal grains; morphology of the grain surface; size and form of grain aggregates (lumps and/or stacks); size and configuration of microcavities within the sample; interrelation of grains, aggregates and cavities or "space filling".

The energy dispersive spectrometer permits to analyse the crystal depicted with an electron signal rapidly for the chemical composition. Thus the correlation of particular morphologic features observed (rods, spheres, cubes, flakes) with their composition can be established. Fig.4.10 shows an example of this kind of application. On the flat surface of an ankerite crystal strange tooth-like protrusions were observed in the SEM image. The Ca content measured by the analysis of the X-ray excited from the very crystals made possible the positive identification of these "teeth" as calcite.

The energy dispersive analysis system using a semiconductor detector and sophisticated electronics measures the energy of the X-rays emitted from the specimen and produces a spectrum of counts versus energy. The spectrum is usually displayed on a video terminal which is equipped with a variety of labels aiding the evaluation. Fig.4.11-A shows a spectrum collected by an EDAX-made instrument. It can be seen that here iron can be identified as a contributor to the spectrum without using any tables, graphs or alike. Exploiting the capabilities of the usually coupled mini computer (semi-) quantitative analysis can be carried out.



Fig. 4.10  
TOTHLIKE CRYSTALLITES ON THE FLAT SURFACE  
OF AN ANKERIT CRYSTAL



- alpha numeric display of
- window number
  - window count rate
  - K L or M level
  - energy of the peak
  - element symbol
  - verify window's resolution
  - background level
  - rate of the peak
  - sample identifier

Fig. 4.11-A  
 TYPICAL VIEW OF THE VIDEO DISPLAY OF AN ED X-RAY ANALYSER.  
 THE LABELS YIELD GOOD MANY INFORMATION



Using the information already available in the images of bauxites selected for SEM investigation, the type, age and geologic history of the deposit can be assessed. E.g. the grain size increases with the pressure due to overburden and compaction is also a sign for high tectonic pressures. Gibbsite, boehmite and other components can be identified referring to their characteristic morphology and texture.

#### TRANSMISSION ELECTRON MICROSCOPY (TEM)

In the majority of bauxites the individual mineral particles are too small to be studied by any instruments but electron microscopes. Fig. 4.11-B shows a particle size histogram typical for Hungarian bauxites. Here the particle dimension falls in the submicron range. (Bars drawn with continuous lines represent the length - while those with dotted contour the width - distribution.)

One of the difficulties in preparing minerals for electron-microscopic studies is to achieve the complete dispersion of the particles. Violent grinding in a mortar with ethyl alcohol or ultra-sound shaking in an appropriate liquid might help to separate the primary units from an aggregate. A drop of the diluted slurry is then allowed to dry on a microscopic sample holder grid covered by a holey carbon film. Fig. 4.12 is the micrograph of a bauxite sample successfully dispersed in some parts of the specimen to observe the distorted hexagonal shape of some individual particles (e.g. that one marked by an arrow). The result of a large number of observations can be summarized that kaolinite usually forms platy crystals, goethite appears needle like, gibbsite and hematite tend to be more isometric and some minerals crystallize in or are crushed to irregular forms. These experiences form the basis of TEM identification of mineral components and the determination of their particle sizes and the form of their aggregation. More definite but also labour some way of identification is to prepare and evaluate electron diffraction photographs. Energy dispersive X-ray analysis can be applied also in TEM to obtain

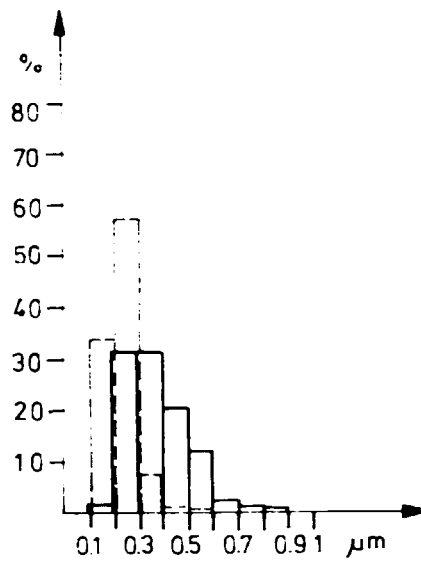


Fig. 4.11-B  
 PARTICLE SIZE HISTOGRAM OF A BAUXITE  
 SAMPLE BASED ON TEM MEASUREMENTS

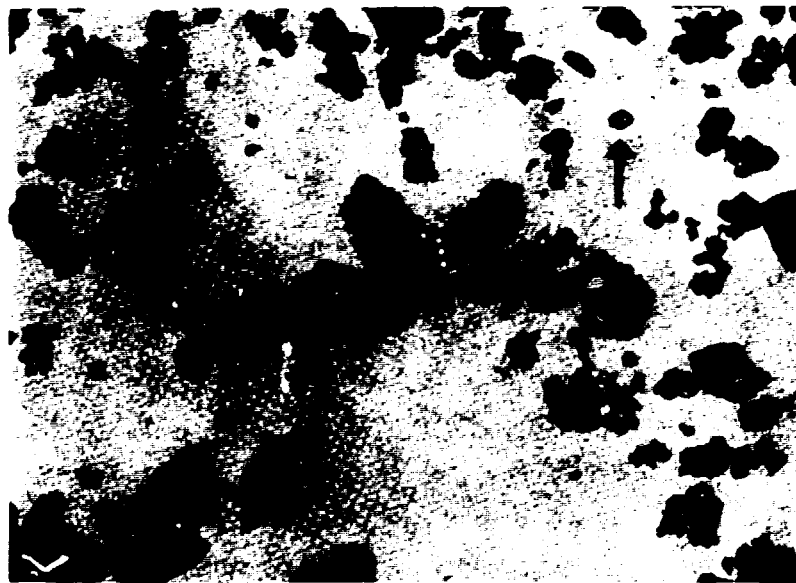


Fig. 4.12  
 ELECTRONMICROSCOPIC /TEM/ PHOTOGRAPH OF A  
 BAUXITE SAMPLE

chemical data on particles as small as some times 10 nm in diameter. It is clear that TEM techniques yield the most detailed information about texture with the highest power of resolution. The shape outline and morphology of the particles - as revealed by electron microscopy - vary to a great extent depending on mineralogical composition and origin of the sample.

The evaluation of texture data from TEM microphotographs can be accelerated a great deal if up-to-date image analysis methods and apparatus is applied. In this case the particle size distribution is calculated and statistically handled by a computer which collects data via an optical digitizer system sensing the coordinates of the perimeters of each particle.

#### MINERALOGIC INVESTIGATIONS

In this chapter the most important methods of identification and quantitative determination of the mineral phases constituting the multicomponent powder mixture called: bauxite are to be described.

This information is of very high importance since as long as bauxite remains the major raw material source for alumina production its mineralogical composition will continue to determine the operating parameters to be employed in Bayer plants. Improving of efficiency and economy by diminishing the specific caustic loss and enhancing the yield of alumina must be based on the knowledge of digestable alumina content as well as the form and quantity of silica present, i.e. on details of mineralogic characterization. Although the methods used for bauxite analysis are described separately in this section it must be noted that in the technological practice crosschecking with the information gained on the corresponding red muds must be carried out.

The minerals that occur in bauxites used commonly in alumina industry are as follows:

Gibbsite	$\text{Al(OH)}_3$	Hematite	$\text{Fe}_2\text{O}_3$
Boehmite	$\text{AlOOH}$	Goethite	$\text{FeOOH}$
Kaolinite	$\text{Al}_2\text{Si}_2\text{O}_5(\text{OH})_4$	Magnetite	$\text{Fe}_3\text{O}_4$
Quartz	$\text{SiO}_2$	Siderite	$\text{FeCO}_3$
Lithiophorite	$(\text{Al,Li}(\text{MnO}_2)\text{OH})_2$	Pyrite	$\text{FeS}_2$
Crandallite	$\text{CaAl}_3(\text{PO})_4\text{OH}_5 \cdot \text{H}_2\text{O}$	Anatase	$\text{TiO}_2$
Chlorites	an extended family of minerals, with compositions similar to e.g.: $10(\text{Mg,Fe})\text{O} \cdot 0.2\text{Al}_2\text{O}_3 \cdot 6\text{SiO}_2 \cdot 8\text{H}_2\text{O}$	Rutile	$\text{TiO}_2$
		Calcite	$\text{CaCO}_3$
		Dolomite	$\text{CaCO}_3$

The full number of mineral species that had been ever detected in bauxites is well over fifty, however, these minor phases are in most cases interesting only from scientific point of view. Here we will regard only processes for the determination of the commercially important mineral components.

#### X-ray Diffractometry

X-ray diffraction has no parallel when the identification of crystalline components of a mixture is to be carried out and its sensitivity/accuracy performance is also excellent for the quantitative determination of many phases.

When a solid is exposed to X-rays of a well defined wavelength (Fig.4.13.) besides the transmitted primary  $I_0$  beam there will appear radiation surfaces of cones of revolution around the incident beam as axis, like the one shown in the figure. When a powder, consisting of a mass of randomly oriented crystallites, is bathed in a narrow pencil of X-rays several cones of so called diffracted beams will be formed. The  $2\theta$  opening angles of these cones and the relative intensities of X-rays in each of these cones define a definite "diffraction pattern" which is uniquely characteristic for

the crystal structure of the sample irradiated. Having measured the  $2\theta$  angle it is fairly easy to calculate the  $d$  spacing of those crystallographic planes which gave rise to the diffracted cone in question:

$$2d \sin \theta = \lambda \quad \text{or} \quad d = \frac{\lambda}{2 \sin \theta}$$

Several compilations are available where the diffraction patterns usually in terms of  $d$  (interplanar spacing) and  $I/I_0$  (relative intensity) values of different materials are systemized to be used for "fingerprint" identification purposes. The most complete file is that published and yearly updated by the Joint Committee for Powder Diffraction Standards (JCPDS). This Powder Diffraction File (PDF) records the diffraction patterns of almost 30,000 materials in 1979 including both organic and inorganic substances. The file is offered for sale in various forms ranging from card files through microfiches to magnetic tapes for computer applications. Search for a definite reference pattern in this huge file is much easier if the number of possible candidates can be diminished by additional evidences (e.g. chemical data, type of material). The mineral subfile (ASTM) consists of only about 5,000 patterns and in alumina technology the use of the latter will be sufficient for the purposes of qualitative analysis.

Diffraction patterns of the individual phases in a mixture simply superpose. Identification becomes the more difficult the higher the number of components is because of the increasing probability of overlapping. Nevertheless, with appropriate techniques usually 10 or even more mineral components of a mixture can be identified reliably.

Thus, in order to carry out mineral phase analysis by X-ray methods the diffraction pattern has to be recorded first. The equipment most commonly used for this purpose is the powder diffractometer including three main parts: 1) X-ray generator, 2) goniometer, 3) electronics (Fig.4.14).

Generators produce radiation by applying a stabilized, quaziconstant potential of about 40-60 kV to a sealed off X-ray tube of 1,5-2,0 kW power. The tubes are water cooled to prevent the melting down of the anode which is generally plated by copper yielding a strong beam at a  $\lambda = 1,54178 \text{ \AA}$  (0,154178 nm) wavelength. A high degree of radiation safety must be provided for because X-rays are harmful to the human body. This is similarly required for the geniometer, where the beam is restricted to well determined directions by collimation (Fig.4.15).

The ideal specimen for X-ray powder diffraction analysis is completely homogeneous over the range of less then 1  $\mu\text{m}$ , has constant particle size of between 1 and 20  $\mu\text{m}$  and showing no preferred orientation or strain. Such a specimen may be difficult to obtain in the practice thus it is important to realize what problems are likely to arise if the specimens deviate from this ideal state.

The actual volume of a specimen analysed is rather small - probably about 2  $\text{mm}^3$ . In addition the penetration of the X-ray beam is also very small, particularly at low angles generally used in bauxite investigations, where it may be as small as a few tens of micrometers. It will be clear from those mentioned above that care must be taken at the sample preparation stage to ensure that the volume analysed would be really the representative of the whole. Where the particle size is large, a problem may arise simply due to particle statistics. Only crystallites having reflecting planes parallel to the specimen surface can contribute to the diffracted in-

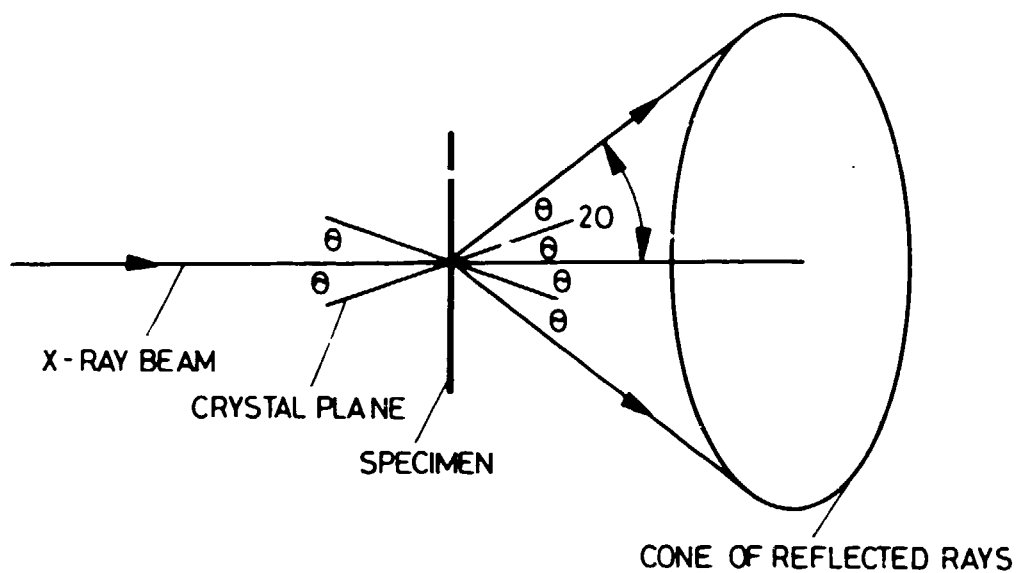


Fig. 4.13

## DIFFRACTION FROM A POWDER SPECIMEN

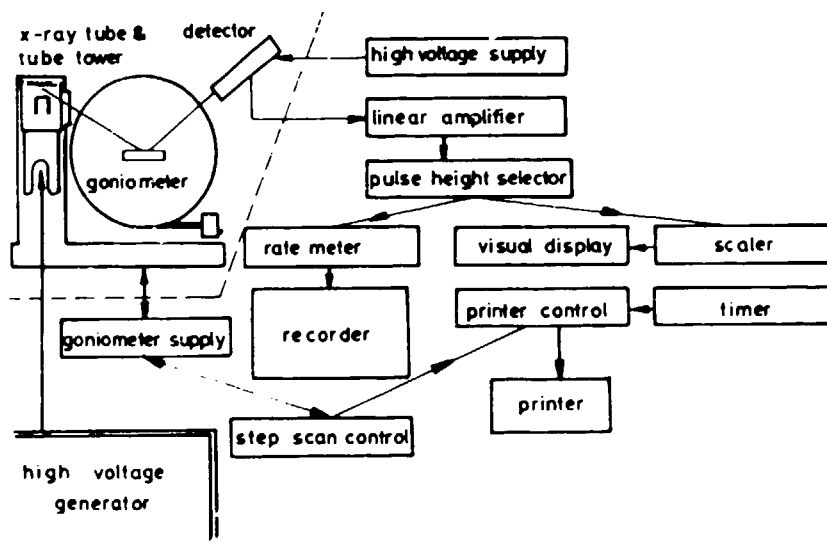


Fig. 4.14

BLOCK DIAGRAM OF A TYPICAL X-RAY  
DIFFRACTOMETER SET-UP

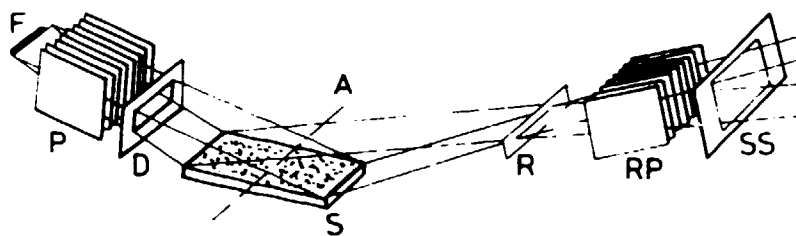


Fig. 4.15

## GEOMETRY OF THE GONIOMETER

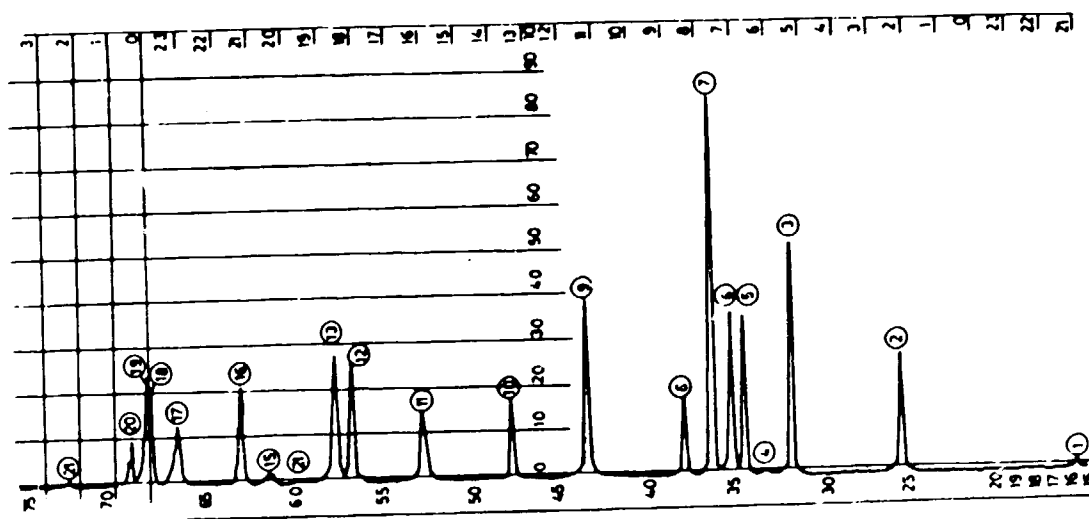


Fig. 4.16

DIFFRACTION PATTERN OF A MIXTURE  
OF  $ZnO$  AND  $Al_2O_3$



tensity and where this number of crystallites is too small to suppose random distribution, an error of the intensity measurement results. Among normal circumstances this error may be as large as 5-10 %. Use of a device allowing the spinning of the specimen in its own plane during the analysis gives a larger effective surface and thus reduces the chance of non-random distribution in the case of preferred orientation where due to the shape of the crystallites it is impossible to obtain random orientation. Specimen spinning will do little to overcome this preferred orientation and the best solution lies in the careful specimen preparation. Most X-ray mineralogists regard as optimal the backloading of powders into the specimen holder usually covered by a material possessing rough surface (e.g. abrasive paper).

The sample is placed onto the goniometer which moves it together with the detector around a common axis during the measurement in an adequate way to obtain good quality diffraction patterns consisting of "peaks" or "reflections" of measurable heights at definite  $2\theta$  positions of the detector. The  $2\theta$  diffraction angles belonging to the peaks can be read from such a diagram directly as the positions of the highest point of each peak or some more sophisticated procedures can be used for their definition, e.g. the mid-point of the cord drawn into the peaks at a definite height (1/2 of the maximal), center of the gravity, etc. The area under the peak gives a better measure for the diffracted intensity than the height. This can be approximated in practical measurements by different methods.

The detector of the goniometer is a proportional or scintillation counter placed after a graphite monochromator which is almost indispensable in taking good quality diffractograms of bauxites. The signal of the detector is fed through some electronics to a recorder producing a diffraction pattern like that shown in Fig.4.16, or a punched tape storing the

digital data of the diffraction measurement which can be further processed by a computer. A still higher efficiency is attained when the goniometer operates under on-line control of the computer which collects and evaluates the data. In this case it seems to be very comfortable if the set of samples is placed in an automatic sample changer handling 30-40 samples without human intervention.

The identification of crystalline phases by X-ray diffraction can be demonstrated using the example of the diffractogram shown in Fig.4.16. In this pattern one can recognize 21 peaks which are enumerated in the order of  $2\theta$  increasing angles. Measuring these angles of diffraction the  $d$  values (interplaner spacings of the corresponding reflecting planes) listed in the second column of the table shown in Fig.4.17 are obtained with the aid of some  $2\theta - d$  conversion tables or a calculator ( $d = \frac{\lambda}{2 \cdot \sin\theta}$  ).

The intensities belonging to each peak can be determined by measuring the peak height along the scale of the strip chart and using the highest amplitude ( $I_0$ ) as a reference for all others expressed in percentages of that ( $I/I_0 \cdot 100$ ). The measured intensities for this case are given in the third column.

Taking the 3 strongest peaks (labelled 9.6 and 2 in this pattern) one can make a systematic search in the Powder Diffraction File for any crystalline compound having the same strongest reflections. Here alpha- $\text{Al}_2\text{O}_3$  can be suspected as giving diffraction identical to a subset of the pattern of Fig.4.16. The complete set of diffraction data for alpha- $\text{Al}_2\text{O}_3$  are to be found on the PDF card 10-173 (Fig.4.18).

Now it can be checked whether all significant reflections of alpha- $\text{Al}_2\text{O}_3$  are present in the observed pattern. This side of the identification seems to be satisfactory. On the other hand there remained some unexplained peaks. The strongest ones

Line	d/Å/	I/I <sub>0</sub>	α-Al <sub>2</sub> O <sub>3</sub>		ZnO	
			d/Å/	I/I <sub>0</sub>	d/Å/	I/I <sub>0</sub>
1	5.68	2.5				
2	3.48	31	3.479	75		
3	2.814	62			2.816	71
4	2.698	2				
5	2.612	42			2.602	56
6	2.557	43	2.552	90		
7	2.482	100			2.476	100
8	2.384	19	2.379	40		
9	2.089	47	2.085	100		
10	1.914	20			1.911	29
11	1.743	19	1.740	45		
12	1.629	31			1.626	40
13	1.605	33	1.601	80		
14	1.549	1	1.546	4		
15	1.514	3	1.514	6		
16	1.478	25			1.477	35
17	1.408	15	1.404	30	1.407	6
18	1.382	(26)			1.379	28
19	1.376	(30)	1.374	50		
20	1.360	11			1.359	14
21	1.340	19	1.337	2		

Fig. 4.17

TABULATED DIFFRACTION DATA FROM ZnO  
PLUS α-Al<sub>2</sub>O<sub>3</sub> /MEASURED FROM THE  
DIFFRACTOGRAM OF FIG. 4.16 /

d	2.09	2.55	1.60	3.48	$\alpha$ -Al <sub>2</sub> O <sub>3</sub>				
I/I <sub>1</sub>	100	90	80	75	Alpha Aluminium Oxide		(Corundum)		
Rad. CuK $\alpha$	1.5405	Filter	Ni Dia	d Å	I/I <sub>1</sub>	hkl	d Å	I/I <sub>1</sub>	hkl
Cut off	I/I <sub>1</sub>	Diffractometer		3.479	75	012	1.1382	2	311
Ref. Nat. Bur. Standards (U.S.)	Circ. 539	9	3	2.552	90	104	1.1255	6	312
(1959)				2.379	40	110	1.1246	4	128
Sys. Triagonal	S.G. D <sub>SD</sub> <sup>6</sup>	-R $\bar{3}$ c	(167)	2.165	<1	006	1.0988	8	0.2.10
a <sub>0</sub> 4.758	b <sub>0</sub>	c <sub>0</sub> 12.991	A C 2.7303	2.085	100	113	1.0831	4	0.0.12
$\alpha$	$\beta$	$\gamma$	Z 6 Dx 3.987	1.964	2	202	1.0781	8	134
Ref. BID.				1.740	45	024	1.0426	14	226
				1.601	80	116	1.0175	2	402
				1.546	4	211	0.9976	12	1.2.10
$\epsilon\alpha$	nw $\beta$	$\epsilon\gamma$	Sign	1.514	6	122	.9857	<1	1.1.12
2V	D	mp	Color	1.510	8	018	.9819	4	404
Ref.				1.404	30	124	.9431	<1	321
				1.374	50	030	.9413	<1	1.2.11
Sample annealed at 1400 °C for four				1.337	2	125	.9345	4	318
hours in an Al <sub>2</sub> O <sub>3</sub> crucible. Spect.				1.276	4	208	.9178	4	229
anal. showed <0.1 % K, Na, Si;				1.239	16	1.0.10	.9076	14	324
<0.01 % Ca, Cu, Fe, Mg, Pb;				1.2343	8	119	.9052	4	0.1.14
<0.001 % B, Cr, Li, Mn, Ni.				1.1898	8	220	.8991	8	410
Corundum structure.				1.1600	<1	306	.8884	<1	235
Pattern made at 26 °C.				1.1470	6	223	plus 11 lines to .7931		

Fig. 4.18

THE PDF CARD OF ALPHA-AL<sub>2</sub>O<sub>3</sub>

of these are again looked for a matching pattern in the PDF. ZnO can account for these. Since these two standard patterns cover the whole of Fig.4.16, it can be taken as identified with a mixture of alpha-Al<sub>2</sub>O<sub>3</sub> and ZnO.

The most simple procedure for determining the percentages of the phases present is to multiply the measured intensities ( $I_i$ ) with appropriate conversion factors ( $k_i$ ) which give how many percentages from a given crystalline phase ( $X_i$ ) correspond to a unit of intensity of a particular reflection.

The PDF gives such intensity conversion factors for a lot of compounds or else they can be determined experimentally. This experiment had been accomplished for bauxites by Bárdossy (1966). Where no reference material is blended to the unknown mixture it must be admitted that the sum of all identified crystalline phases correspond to the total quantity of the sample

$$\left( \sum_{i=1}^n X_i = 100 \% \right).$$

Percentages of the individual phases are then obtained using the following simple and symmetrical formula:

$$X_i = \left( \frac{k_j}{k_i} \sum_{i=1}^n \frac{I_i}{k_i} \right)^{-1}$$

The sensitivity for a component  $i$  in a given sample is defined as the rate of change in net signal output  $I_i$  to concentration increment,  $X_i$  (%). This is given for the X-ray analysis by:

$$S_i = k_i \sum_{i=1}^n \frac{I_i}{k_i}$$

The detection limit for a component  $i$  in a given sample is defined as the minimum concentration,  $X_i$  (%), required to give an observable signal,  $I_i$ , which is usually taken as three standard deviations of the background intensity,  $3\sqrt{I_b}$ . Hence the detection limit for component  $i$  in a sample by the X-ray diffraction technique is:

$$X_i(\text{det. lim.}) = \frac{3\sqrt{I_b}}{S_i t}$$

where  $t$  is the time used for the background.

The X-ray diffractogram may yield information about the structural details, too. The determination of unknown atomic arrangements requires measurements on single crystals, however, in order to detect slight differences between arrangements realized along the same basic model, accurate powder data are sufficient. This was proved recently several times using the method of pattern fitting structure refinement (PFSR). This method needs rather big computer capacities.

Evaluation of the breadth of the powder diffraction peaks offers some additional information about the dispersion and distortion of the crystallites. This can be understood recalling that a particular setup provides the sharpest diffraction peaks when the crystallites possess perfect lattice order and their sizes are about 0.1-5  $\mu\text{m}$ . Defects in the lattice (strain, dislocations, etc.) as well as particles smaller than 0.1  $\mu\text{m}$  (100 nm) cause broadening of the peaks. Unfortunately these two effects can not be simply separated from the informations gained by measuring the broadening of the peaks. However, in some cases it might be justified that all the broadening should be regarded as due to particle size effects.

Then the relationship

$$D = \frac{\lambda}{\beta \cos \theta}$$

can be used to calculate the mean crystallite dimensions (D) perpendicular to the reflecting planes corresponding to the peak evaluated for broadening ( $\beta$ ). K is a constant, which has usually a value of about 0.9 ;  $\lambda$  is the wavelength of the radiation applied;  $\theta$  is the angle of diffraction.

#### THERMAL METHODS

Several properties of minerals like chemical composition and bonding change when they are exposed to heat treatment. In thermal investigations the sample is placed in a controlled atmosphere and various parameters characterizing the physical-chemical state of the sample are measured or recorded as a function of the temperature varied according to a predetermined program. The most frequently used methods of thermal analysis are differential thermal analysis (DTA), thermogravimetry (TG) and differential thermogravimetry (DTG). Dilatometry and other thermal methods will not be concerned here because they have only secondary role in the bauxite analysis.

Differential thermal analysis (DTA) is a technique in which the temperature difference between a substance and a reference material is measured as a function of temperature whilst the substance and reference material are subjected to a controlled temperature program.

Thermogravimetry (TG) is a technique in which the mass of a substance is measured as a function of temperature whilst the substance is subject to a controlled temperature program.

The technique of differential thermogravimetry (DTG) is almost the same as that of TG, here the change is purely of mass per unity temperature variation  $\Delta G/\Delta T$  plotted versus the temperature. DTG curves help to define the exact temperature, where the rate of mass change is experienced to be the highest.

DTA, TG and DTG measurements can be carried out each by a separate instrument designed particularly for that kind of thermal investigation, or else, by an equipment permitting the simultaneous recording of any two or all three types of thermal curves. Among other combined thermogravimetric instruments the "Derivatograph"-s developed by L.Erdey-F.Paulik and J.Paulik and manufactured by MOM, Budapest, have been frequently used in alumina technology both in R and D connected studies and in plant control, too.

The main parts of any setup used for thermal analysis are: heat source, temperature regulating system, specimen holder and block, temperature measuring and recording system, mass measuring and recording system (microbalance), apparatus to produce vacuum or maintain a desired atmosphere.

A DTG curve can be obtained e.g. if the sample is heated in a furnace at a constantly increasing temperature while suspended from the pan of the balance to the lever of which a permanent magnet is attached moving freely inside a solenoid. When a change of weight occurs the magnet moves and the current generated in the solenoid is recorded by means of a recording drum. Nowadays this analogue way of differentiating is usually replaced by digital data processing, where the TG data are differentiated using on-line or off-line computer capabilities.



Apart from being influenced by differences in apparatus, the thermal curves are particularly sensitive to variations in technique. Therefore all parameters which effect the changes occurring upon heat treatment should be carefully controlled in the laboratory practice and exactly stated in reports and publications. Compatible results can be expected from experiments carried out at different places only if the instruments are designed according to common principles and standard procedures (including preparation of the specimen, size of the specimen, heating rate, positioning of the thermocouples, material of the crucibles, etc.) are applied.

In the mineralogical investigation of bauxites thermal methods are used in order to gain complementary information to those obtained by other methods. Some important components of bauxites, like hematite, rutile, anatase, quartz and the anhydrous alumina oxides possess no or only very slight diagnostic thermal criteria over the normally used temperature range of 0-1.000 °C. However, for some components thermal analysis yields outstanding possibilities of identification and quantitative determination.

Thermogravimetry and differential thermogravimetry are based upon weight changes. When heating bauxite samples one could expect weight change due to loss of absorbed water, bound or crystalline water (dehydration), decomposition of carbonate, sulphate, sulfide, phosphate phases or organic components. The start point of these reactions as revealed from the weight loss curves as well as the similarly detected temperature of maximum rate and the end point of the reactions are characteristic for the phases involved. Therefore they can be used to identify the components of bauxites and determine their quantities. It must be, however, also taken into account that gain in weight is possible e.g. when heating sulphates in air and the metal resulting from the decomposition oxidizes.

In differential thermal analyses the difference in energy absorbed or released by the sample and the reference material, respectively, is sought for. When reactions occur in any material energy is absorbed (endothermic events) or evolved (exothermic events), irrespective of whether or not there is a weight change. Thus differential thermal analysis based on measuring energy changes has the advantage that it can detect such events like recrystallisation, crystal inversion, structural transformations, etc. in addition to reactions involving weight change. Curves obtained for energy changes are inherently less quantitative as those involving weight changes, since factors like thermal conductivity and diffusivity are involved in determining the magnitude of the effects observed. Nevertheless, with suitable safeguards quantitative applications are also possible.

All the curves described may be recorded as well during the cooling cycle, however, this device of checking reversibility of reactions is not very frequently used in the applications to alumina technology.

Determination of quantities can be accomplished after calibration of the instrument in question used under reproducible conditions by means of standard samples. Effective methods were established by several research workers for the measurement of gibbsite, boehmite and diaspore, kaolinite, goethite, calcite, dolomite and pyrite content of bauxites (E.g. Kotsis /1974/).

Differential calorimetry is another method based on energy changes and Quinson, Murat and Bouster stated in a report (1976) that it is more accurate in the quantitative phase analysis of bauxites than the usual thermal methods.

The weight loss curves can be used directly to determine the quantity of water or other identified volatile components leaving the sample. In order to identify precisely the gaseous products sometimes the thermal apparatus is completed by a mass spectrometer or other means of gas analysis.

Let us deal now systematically with the problems of thermal analysis as regards the main mineralogical groups of bauxite constituents.

#### Aluminium Minerals

In this group gibbsite, boehmite and diaspore are found.

DTA and DTG curves for gibbsite ( $\text{Al}(\text{OH})_3$ ) show a strong endothermic peak between  $320^\circ\text{C}$  and  $330^\circ\text{C}$  corresponding to the change of  $\text{X-Al}_2\text{O}_3$  and the peak temperature changes very little if at all with particle size. In addition to this main peak there appear two subsidiary small endothermic peaks at about  $250\text{--}300^\circ\text{C}$  and  $525^\circ\text{C}$ . The temperature of the first peak is usually lower for synthetic samples, about  $250^\circ\text{C}$  and somewhat higher for natural ones:  $275\text{--}300^\circ\text{C}$ . Therefore the second peak may appear either as a discrete maximum or as an inflexion on the main peak.

Research workers agree that the main characteristic of gibbsite DTA is the strong endothermic peak at about  $320^\circ\text{C}$  and DTG as well as TG evidences support the view that the peak at about  $250\text{--}300^\circ\text{C}$  is due to the formation of some boehmite while the other peak at  $525^\circ\text{C}$  indicates the dehydration of the latter. Accordingly weight loss is separated in three steps, the second of which is the most important. For accurate quantitative measurement of gibbsite by DTA high levels of goethite can be disturbing due to the partially overlapping peaks.

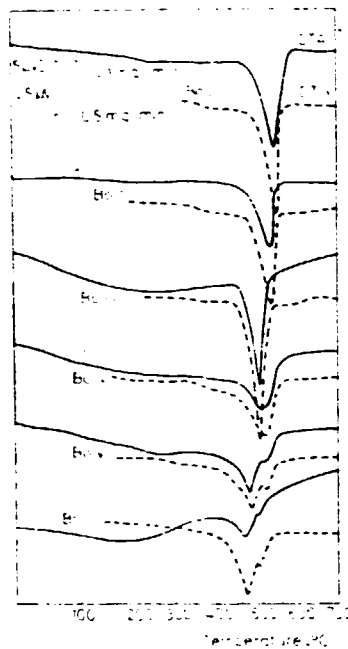
Fig. 4.19 shows simultaneously recorded DTA and DTG curves of six boehmite samples of different origins. As it can be seen from the evaluated peak temperatures, the two sets of thermal observations give consistent data with substantial scattering.

Literature gives for the temperature value of the single endothermic peak of boehmite at 510-560 °C with the average of 510 °C (Mackenzie, 1957). The boehmites belonging to the group of Fig. 4.19 were synthetically prepared with high dispersion, therefore there are still lower values. Thermal investigations tend to support the opinion that porosity has a strong effect on the peak temperature, because the water can be released from the particles easier (at a lower temperature) if there are internal free paths in form of cracks, pores. The two peaks for Bo VI are probably due to two different populations of particles characterized by different porosity. Fig. 4.20 shows thermal curves for a diasporite sample.

The DTA curve exhibits a broad endothermic peak at about 560 °C. The  $H_2O/Al_2O_3$  ratio plotted against temperature reveals that the sample contained more water above this temperature than required by the formula  $Al(OH)_3$ . This was proved to be due to occluded water (11 %) in the fairly large diasporite crystals. Determination of occluded water may be important in several instances in the alumina technology. Diasporite itself loses its water at 560 °C which is indicated by an endothermic DTA peak and a negative DTG peak. This temperature agrees well with those quoted in the literature, viz. 540-585 °C (Mackenzie, 1957).

#### Iron Minerals

Referring to bauxite studies the most important of all iron compounds is goethite ( $FeOOH$ ). It deserves particular interest since it had been proved that substitution of up to



Sample	Peak DTG	temperature DTA	°C
Bo I	540	530	
Bo II	520	520	
Bo III	498	498	
Bo IV	510	500	
Bo V	480	470	
	510	502	
Bo VI	460	455	
	495	490	

Fig. 4.19  
SIMULTANEOUS DTA, DTG OF BOEHMITES

33 mol % of the Fe for Al is possible to show up in the lattice of goethite. The single peak of the DTA, DTG curves is shifted according to the Al substitution in alumogoethites (Solymár and Kenyeres, 1970):

Temperature of peak, °C	310	325	340	355	370	385	400
Mol % Al substitution	0	5	10	15	20	25	30

Fig. 4.21 represents the thermal curves of a Jugoslavian bauxite taken by means of a Paulik-Paulik-Erdey type MOM made Derivatograph. The goethite content is low (about 1 %) while the Al substitution is high (about 20 %).

Should the determination of goethite in a bauxite sample be rendered difficult because of the interfering gibbsite peaks, goethite can be determined in the corresponding red mud and its percentage in the initial sample is then calculated from the chemically determined ratio of the  $Fe_2O_3$  contents. This procedure is based on the fact that alumogoethite is not attacked by the caustic liquor below 240 °C.

#### Silica Minerals

In bauxites there might be present several silica minerals. Quartz does not give thermal effects in the usual range below 1000 °C. Chlorites are less frequent than kaolinite, however, they have characteristic but rather complicated thermal curves.

Kaolinite exhibits an endothermic peak in DTA at about 570 °C and the corresponding weight loss appears between 560-680 °C. The determination of kaolinite is more advantageous from the red mud where the silica content shows up as trans-

4-47

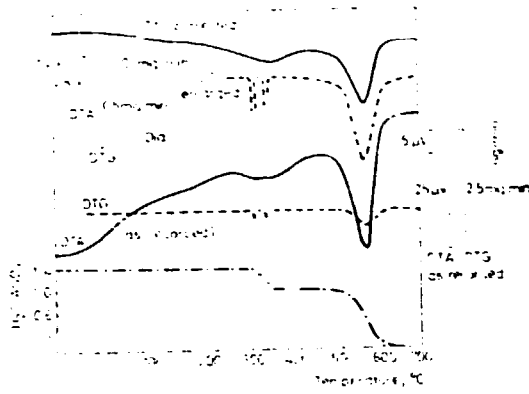


Fig. 4.20

SIMULTANEOUS TG, DTA OF DIASPORE

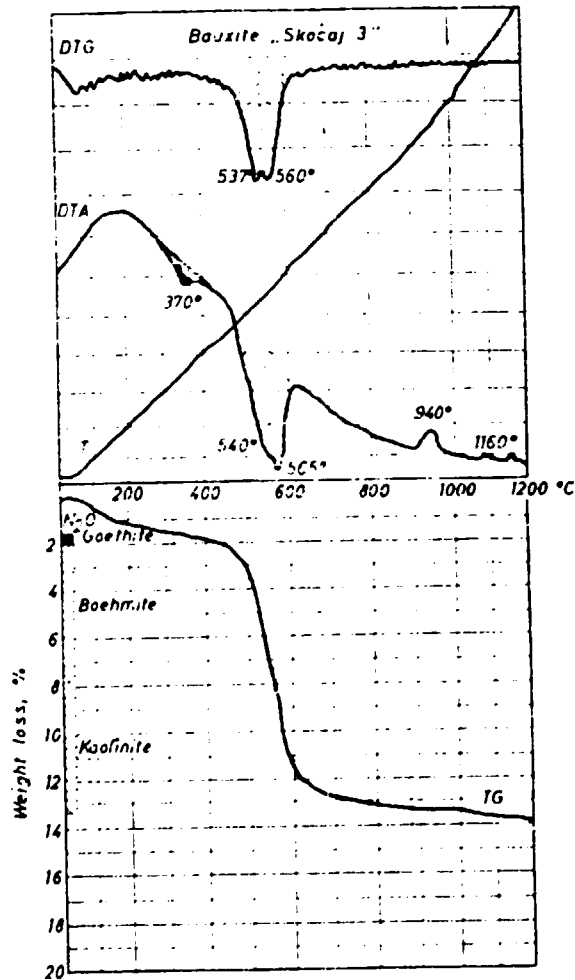


Fig. 4.21

„DERIVATOGRAM“ OF A GOETHITIC BAUXITE SAMPLE

formed to sodalite. This is especially true if boehmite and kaolinite are coexistent. Serious mutual interference is then caused by the fact that the dehydration reactions are almost isothermal for these two minerals. Another approach that has been reported as successful (Sabiston, 1975) is to resort to a controlled atmosphere furnace assembly and expose the sample to positive pressure. This has the effect of displacing the kaolinite dehydration towards higher temperatures without changing the position and size of the boehmite endotherm.

#### Other Minerals

Pyrite gives complex thermal effects. The endothermic reaction in oxidizing atmosphere begins at about 350 °C and peaks appear around 440 °C, 550 °C and 610 °C. Nevertheless, pyrite can be detected very sensitively by thermal methods, i.e. percentages as low as 0.2 w% can be identified.

The mean value published for the characteristic peak of calcite ( $\text{CaCO}_3$ ) is 954 °C. Particle size and crystal size have important influence.

Dolomite ( $\text{CaMgCO}_3$ ) shows less variation in the peak temperatures of both its peaks. Averages values are 790 °C and 940 °C.

#### INFRARED (IR) ABSORPTION SPECTROMETRY

Several minerals of bauxite have structures which include hydroxyl groups with protons in a unique environment and these may be directly examined by infrared spectrometry.

This method of instrumental physical-chemistry is based on the fact that the absorption of radiation takes place in solids at particular frequencies characteristic for the states of chemical bonds in the material. In the  $1-10^4$   $\mu\text{m}$



range of wavelength - infrared region - absorption is due to the change in vibrational or rotational state of the molecules. Commercially available IR spectrometers work in a more restricted wavelength range of 2-200  $\mu\text{m}$ , however, the latest apparatus exploiting the principle of Fourier transformation spectrometry, cover almost the entire spectrum of interest.

Important applications of IR spectrometry are the identification of minerals, their quantitative phase analysis in mixtures using the characteristic absorption bands, the determination of water content in materials as well as the study of bond strength (e.g. that of hydrogen bridges) by means of measuring precisely the shifts of certain IR bands. For the sake of such studies usually laboratory made sets of samples and natural minerals are compared. Identification of standard spectra (e.g. Farmer, 1974).

When mineralogical investigations are extended to more subtle details of the structure IR spectrometry can contribute a great deal to the results gained by other methods. For this purpose first of all the absorption bands have to be assigned to well defined vibrations. A helpful technique in this respect is deuteration. When the hydrogens of OH, H<sub>2</sub>O, H<sub>3</sub>O<sup>+</sup> or other groups are exchanged for deuterium the bands corresponding to vibrations relevant to these entities, and only these, will be shifted. Various chemical and thermal reactions can also be used to identify some of the band and assign them to definite bonds. Thereafter shifts of the bands, change in their intensity and shape might be interpreted in terms of structural modifications.

Basic parts of an IR spectrometer are: source of radiation, specimen chamber, some device permitting spectral resolution (prism, grating or interferometer), detector, recorder or data processor.

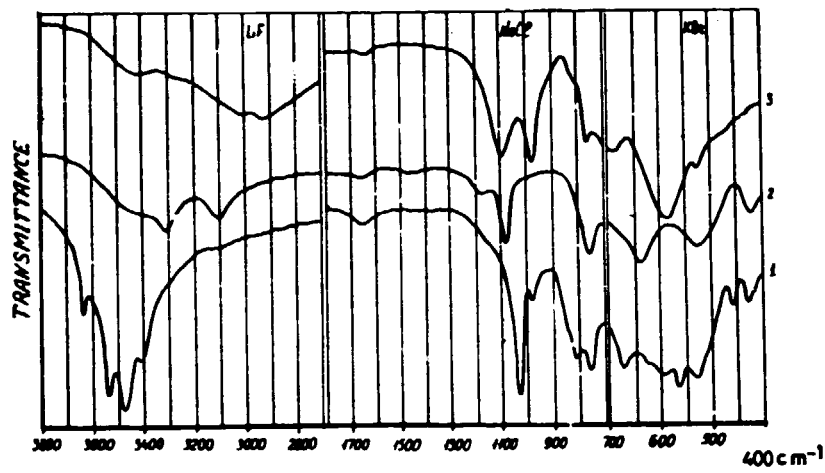
Powder samples are usually pelletized for IR studies. The pellets are prepared under high pressure in special moulds from a mixture of 2-3 mg substance under test and about 600-800 mg KBr.

Fig.4.22 shows standard IR absorption spectra of some pure aluminium mineral phases of bauxites.

The characteristic frequencies of frequently encountered bauxite minerals are as follows:

Kao	Boe	Gib	Goe
750	750	755	<u>800</u>
790		800	
<u>918</u>		840	<u>897</u>
940		975	
<u>1015</u>	<u>1080</u>	<u>1030</u>	
<u>1039</u>			
1110	1155		
	<u>3100</u>		3130
	3290	3385	
		3400	
3628		<u>3455</u>	
3658		<u>3530</u>	The underlined
<u>3700</u>		3625	bands are strong ones.

The lattice vibrations of the various  $AlO_x$  units appear in the 700-800  $cm^{-1}$  wave number range, while the bands of the Al-O-H deformation vibrations and the Si-O stretching vibration are found between 800 and 1200  $cm^{-1}$ . The bands of higher wave numbers belong to the stretching vibrations of O-H groups participating in hydrogen bridges.



1. GIBBSITE
2. BOEHMITE
3. DIASPORE

Fig. 4. 22

ABSORPTION IR - SPECTRA OF THE MAIN  
BAUXITE - FORMING MINERALS

Fig.4.23 shows the IR absorption spectrum of a Haitian bauxite in two wave number ranges together with the identification of the bands corresponding to gibbsite, boehmite and kaolinite.

Fig.4.24 gives spectra for a Jamaican bauxite with less, but still pronounced amount of boehmite besides gibbsite. Bauxites having over 1 % boehmite are unacceptable for low temperature (140 °C) Bayer plants since these are designed for dissolving only gibbsite. This can make understandable the significance of detecting low percentages of boehmite in bauxites by IR spectrometry.

Additionally to the establishment of acceptability or unacceptability of a given bauxite for a particular processing plant by semi-quantitative estimates of the boehmite content, the "reactive silica" component of these bauxites can be determined, too.

Jónás and Solymár (1970) showed that for the simultaneous quantitative determination of kaolinite, boehmite, gibbsite percentages and the modules

$$(m = \frac{\sum Al_2O_3}{\sum SiO_2} )$$

of bauxites the bands at 3100 (boehmite), 3455 (gibbsite) and 3700  $cm^{-1}$  (kaolinite) can be used most successfully. The specific extinction defined as the extinction ( $E = \log I_0/I$ , see Fig.4.25) referred to the grams of bauxite in the pellet (E/g-bauxite) was found to be a good measure of the percentages of the mineral components.

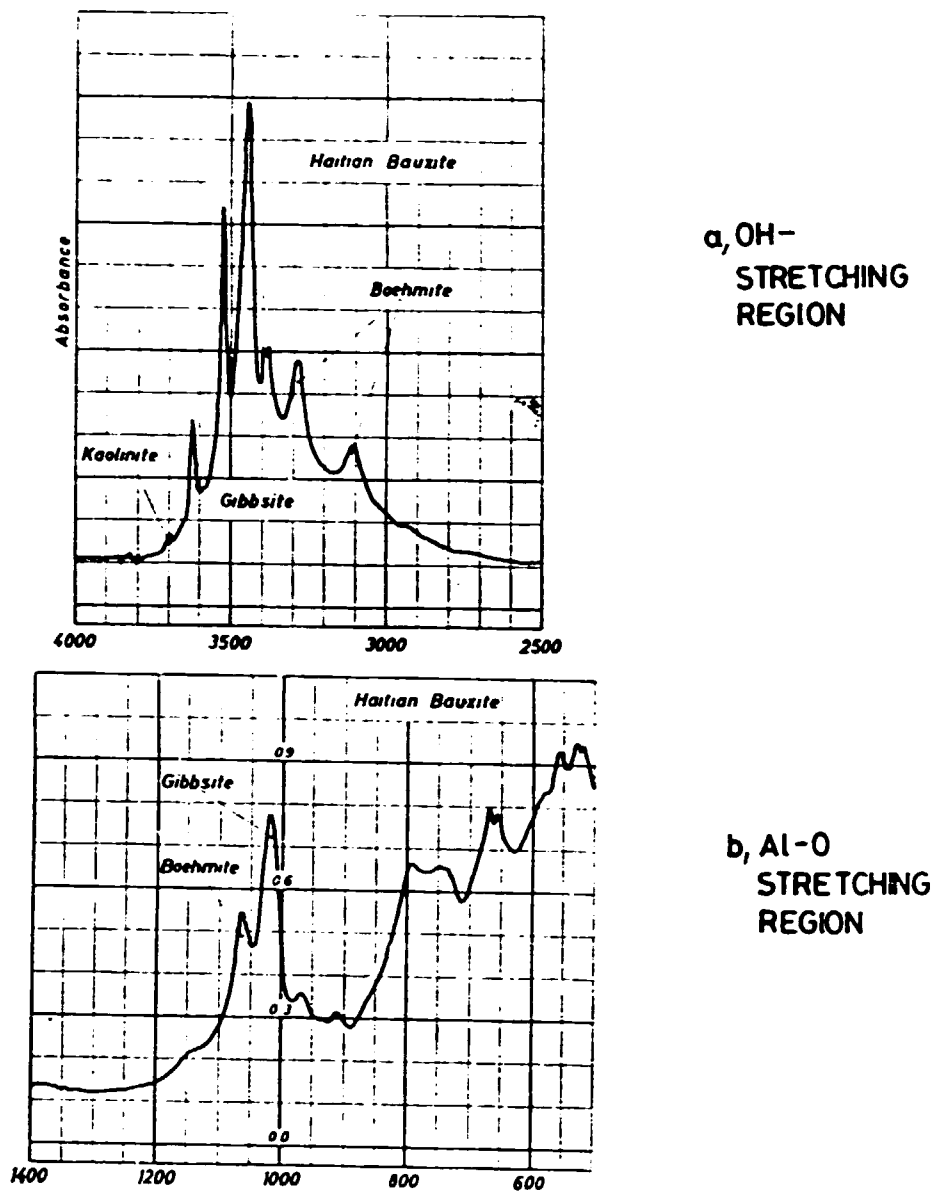
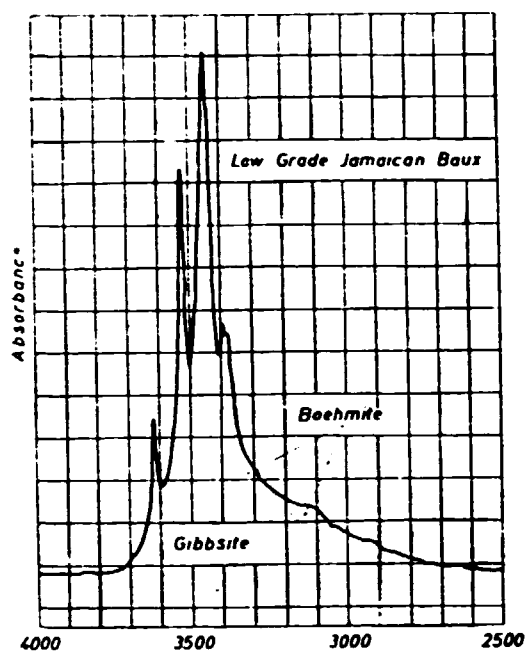
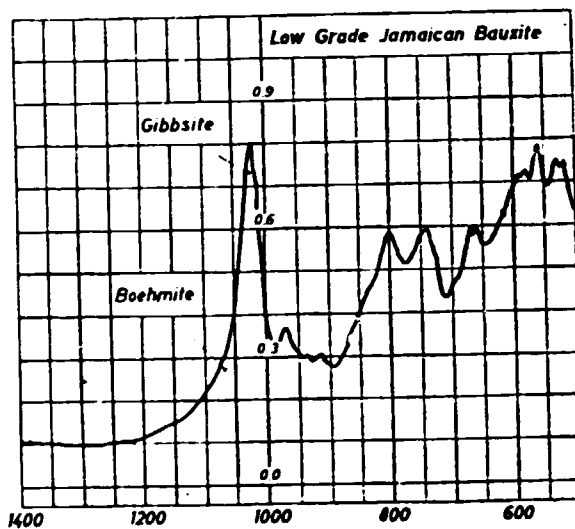


Fig. 4.23

INFRARED SPECTRA OF HAITIAN BAUXITE



a, OH-  
STRETCHING  
REGION



b, Al-O  
STRETCHING  
REGION

Fig. 4. 24  
INFRARED SPECTRA OF LOW- GRADE  
JAMAICAN BAUXITE

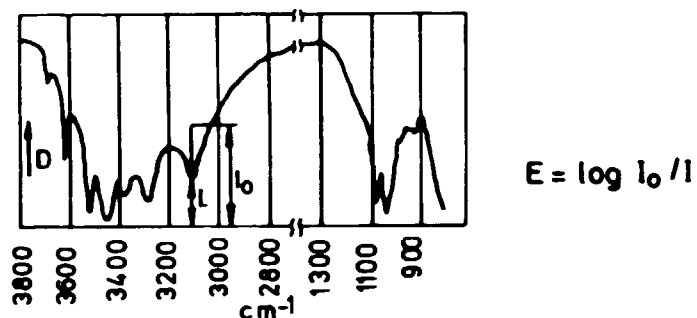


Fig. 4.25

DEFINITION OF IR EXTINCTION, DETERMINATION  
OF THE BASELINE IN AN IR ABSORPTION SPECTRUM

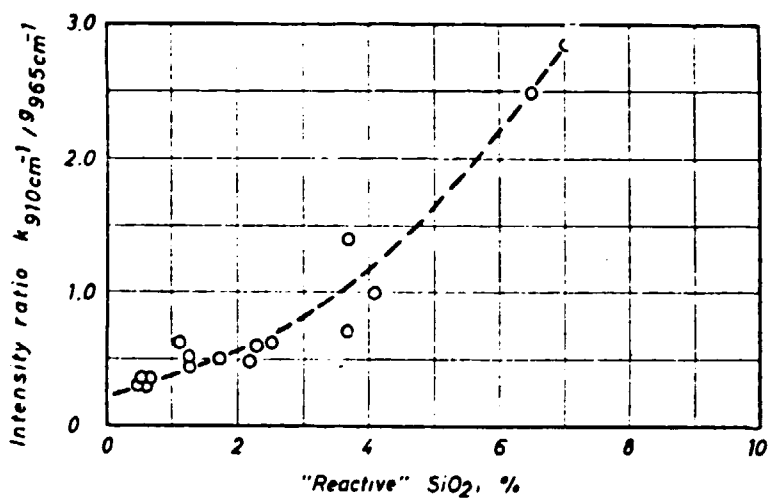


Fig. 4.26

RELATIONSHIP BETWEEN "REACTIVE" SiO₂ %  
AND THE INTENSITY RATIO  $k_{910\text{cm}^{-1}} / g_{965\text{cm}^{-1}}$

Since significant deviations may exist between the intensities of the individual bands of bauxites of different origin, which is due apparently to the differences in their structure, particle size, degree of crystallinity, etc., the calibration curves "percentage of mineral component versus specific extinction" can be applied only to ores of a particular deposits. In this case the error in the kaolinite determination is  $\pm 1.7\%$   $\text{Al}_2\text{O}_3$ , while  $\pm 1.5\%$   $\text{Al}_2\text{O}_3$  in the gibbsite determination and  $\pm 4.6\%$   $\text{Al}_2\text{O}_3$  in the boehmite measurement.

However, experience proved that the error is significantly larger if calibration based on a definite deposit is applied for other bauxites. In order to eliminate this problem the relative intensities were introduced. According to this method the sum of the specific extinctions  $\left[ \sum_i (E/g\text{-bauxite})_i \right]$  of all significant bands in the infrared spectra and the relative contribution of each band to the total absorption was calculated. The calibration curves plotted as this relative intensities against the quantity of mineral phase present in the bauxite were found to be satisfactory even for samples of random origin.

In the work of Jónás and Solymár (1970) the "reactive  $\text{SiO}_2$ " is determined via the  $(\text{Al}_2\text{O}_3)_{\text{kao}}$  indirectly in order to be able to calculate the module. White (1974) described another method useful when kaolinite is the major source of "reactive  $\text{SiO}_2$ ". The intensity ratio  $\text{kao}_{910 \text{ cm}^{-1}} / \text{gib}_{965 \text{ cm}^{-1}}$  for the characteristic kaolinite and gibbsite bands, respectively, may be used as a semiquantitative estimate of the kaolinite. When this ratio is plotted versus "reactive  $\text{SiO}_2$ " a distinct trend can be established for the relation between the amounts of "reactive  $\text{SiO}_2$ " and the kaolinite content (Fig.4.26).



Taking 5 % reactive silica as the upper limit for bauxites acceptable for Bayer plants, any bauxite having an intensity ratio  $\text{kao}_{910 \text{ cm}^{-1}} / \text{gib}_{965 \text{ cm}^{-1}} \geq 1.5$  would be inappropriate for processing.

The presence of kaolinite in bauxites is also manifested by the development of a shoulder at about  $1100 \text{ cm}^{-1}$ . Fig.4.27 shows the infrared spectra of five bauxite samples with total  $\text{SiO}_2$  contents ranging from 0.83 % to 20.72 %. It can be seen that as the  $\text{SiO}_2$  percentage increases the intensity of bands at 3695, 1100 and  $910 \text{ cm}^{-1}$  increase simultaneously. The intensity ratio  $\text{gib}_{3520 \text{ cm}^{-1}} / \text{kao}_{3620 \text{ cm}^{-1}}$  decreases with an increasing  $\text{SiO}_2$  and kaolinite content relative to the amount of gibbsite.

Another important mineralogical application of IR spectrometry in the field of bauxite analysis is the determination of Al/Fe substitution in goethite.

Fig.4.28 illustrates the changes occurring in the IR absorption spectra when Al substitutes the Fe in the goethite lattice. The evaluation of these spectra revealed changes both in the specific extinction and the shifts of the bands. The latter is more suitable for the determination of the Al content of goethite because it seems to be less sensitive to grain size effects, hematite content and other parameters of preparation (Jónás and Solymár, 1970). (Fig.4.29).

The shift of the absorption peaks yields information about the bond strength and reactivity of minerals. Boehmite can serve as an interesting example in this respect. When the band near the wave number  $1085 \text{ cm}^{-1}$  is shifted towards lower values this reflects stronger H-bonding and vice versa. Fig.4.30 gives the relationship between boehmite yield (solubility) and the position of the above mentioned boehmite band for various bauxites (Solymár and Jónás, 1974).

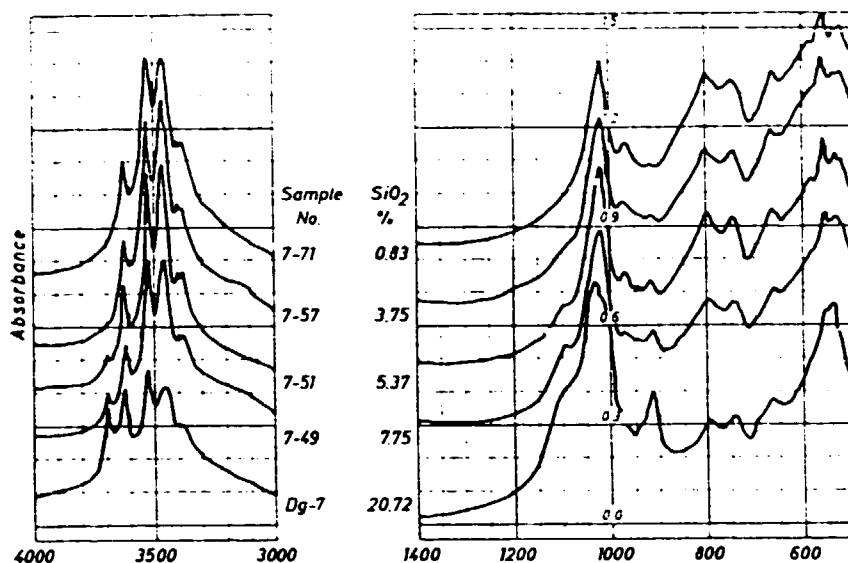
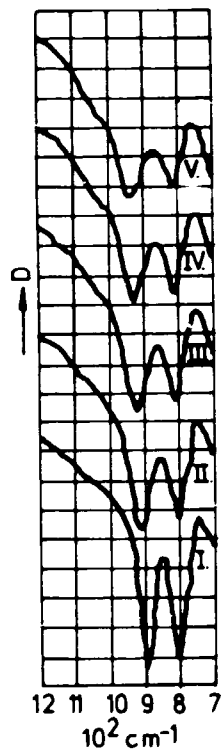


Fig. 4.27

### INFRARED SPECTRA OF BAUXITES WITH RANGE OF TOTAL $\text{SiO}_2$ CONTENT



#### ALUMINIUM CONTENT IN THE SAMPLES

SAMPLE	MOLE %
I.	0.
II.	13.4
III.	15.3
IV.	20.2
V.	22.0

Fig. 4.28

### INFRARED ABSORPTION SPECTRA OF ALUMOGOETHITES IN THE $700\text{-}1200\text{ cm}^{-1}$ WAVE NUMBER RANGE

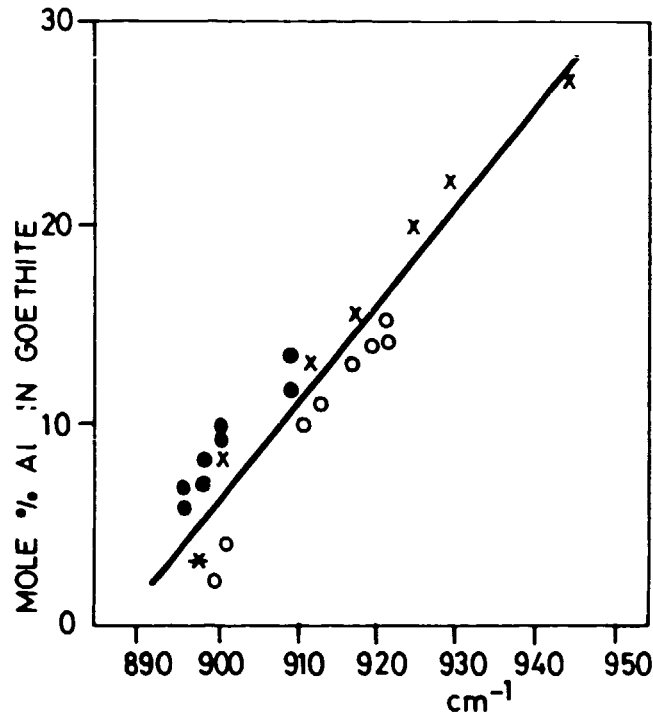
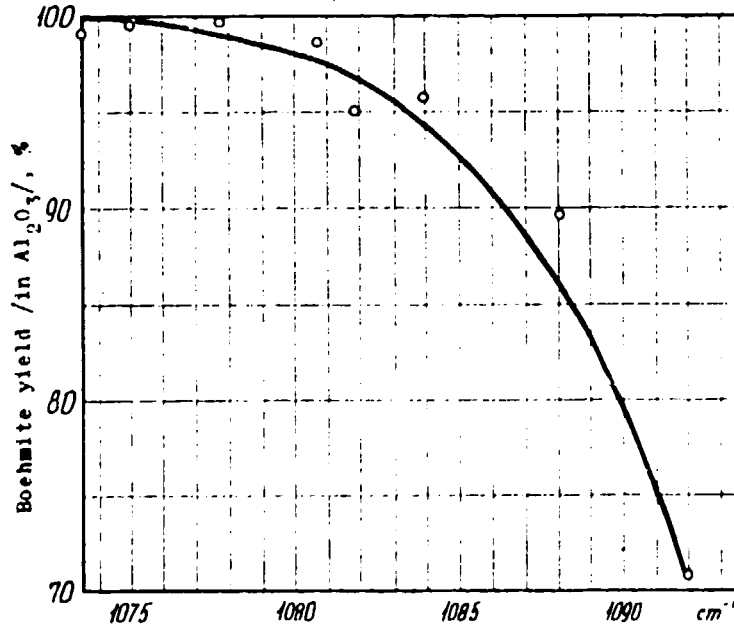


Fig. 4.29

THE SHIFT OF WAVE NUMBER FOR THE GOETHITE BAND NEAR  $900\text{cm}^{-1}$  vs. ALUMINIUM PERCENTAGE



DIGESTION  
AT  $210^{\circ}\text{C}$   
FOR 0.5 h

Fig. 4.30

THE  $\text{Al}_2\text{O}_3$  /BOEHMITE/ YIELD OF VARIOUS BAUXITES AS THE FUNCTION OF THE WAVE NUMBER CORRESPONDING TO THE BOEHMITE BAND

## PARTIAL DISSOLUTION TESTS

Most of the serious difficulties experienced during the mineralogical analysis of bauxites arose from the fact that this ore has a great number of components (10-15). This results in certain disadvantages in the course of almost all experimental procedures applied to bauxites.

Several examples may be referred to in order to support the above statement.

For example it is very difficult to achieve by means of grinding uniform dispersion in a bauxite sample because of the different hardness, cleavage and breaking characteristics of the components what results in smearing and very small particle size in respect of some minerals (boehmite, kaolinite, etc.) and almost no or very slight decrease in particle size of others (rutile, quartz) and, of course there is a third group of intermediate behaviour.

In methods of identification and quantitative analysis of the components, where the basic information takes the form of an intensity or amplitude distribution-curve the overlapping of the maxima of the individual components presents often difficulties.

One way of diminishing the number of components in a bauxite sample in order to avoid these problems is to dissolve selectively a definite part of the contributing minerals. However, caution is required to ensure the insolubility of the mineral(s) being sought.

Gibbsite and kaolinite are readily attacked by sodium hydroxyde whereas the caustic solubility rate of boehmite is relatively low. By increasing the  $\text{Al}_2\text{O}_3$  content of a sodium aluminate solution to the level of boehmite saturation,

this reagent can be used to remove gibbsite and clay minerals, leaving alumina monohydrate mineral(s) as well as titania and Fe-minerals in their original state.

For ferruginous bauxites the removal of iron minerals can often reveal hitherto undetected mineral phases. Use of classical nascent hydrogen reduction or the sodium dithionite procedure is equally effective for the selective leaching of hematite and goethite.

Boiling for half an hour in 10 % chloric acid removes also the majority of the iron minerals, while aluminium, titanium and clay minerals remain unchanged.

Selective solvent, their concentration, temperature and time of application or other parameters of the dissolution test must be specifically experimented for each aim to be accomplished. Before the final conclusions are drawn true selectivity should be critically checked.

Both the solid residue and the dissolved component can be determined if systematic measurements are made before and after the dissolution steps. Taking for example the difference of the IR absorption spectra of the untreated sample and the one subjected to the selective solvent, the resulting difference spectrum corresponds to the missing dissolved component(s). Experimentally, such difference spectra can be taken easiest if a two beam spectrometer is used and each of the samples to be compared is placed into one of the beam.

Selective dissolution may be also very useful in X-ray diffractometry to get rid of the confusing interferences and enhance thereby the sensitivity, as it will be explained later.

## MÖSSBAUER SPECTROMETRY

Mössbauer spectrometry is perhaps the youngest method of materials research finding its way to mineral characterization in the alumina industry. Since it is specifically bound to the presence of  $^{57}\text{Fe}$  ions it can be used only to study the properties of iron minerals or other ones which are stained with iron.

Mössbauer spectroscopy is a valuable adjunct to X-ray diffraction for defining the nature and distribution of iron-bearing constituents (E.g. Hogg, Malden and Meads, 1975). A paper of Janot and Gilbert (1970) provides data on iron minerals not obtainable by other mineralogical techniques. Mössbauer spectroscopy afford data on the coordination of  $^{57}\text{Fe}$ , its valency state, magnetic state and even information on crystallite size ( $< 20$  nm) beyond the capabilities of X-ray diffraction. An example of such study can be found in the paper of Jefferson, Tricker and Winterbottom (1975). The aim of this research was to determine whether  $^{57}\text{Fe}$  substituted in the kaolinite lattice for Al formed a more or less amorphous surface layer or was present as small crystalline goethite particles stuck to the surface. Investigating nine kaolinite samples from a variety of locations the different kinds of iron contaminations could be separated as well as specific ways could be recommended for cleaning the samples from iron, if possible. Attached fragments of goethite and thin amorphous coatings could be easily removed by acid extraction, but the substituted iron, occupying sixfold coordinated positions in the kaolinite lattice could not be attacked by this way.

The concentration and arrangement of iron in aluminium-hydroxides can be determined by this technique and undoubtedly its role will be increasing in the future studies on bauxite minerals.

#### OPTICAL METHODS

Mineral particles are generally identified using a polarizing microscope. Mineral particles of the main components of bauxites are in most cases too small to be studied in microsections using microscopic methods. Thus such studies are restricted to the larger particles (quartz, zircon, etc.) and to specially separated microminerals.

The term "micro-mineralogical test" involves in the practice the investigation under the microscope of individual mineral particles with dimensions exceeding (0.06 mm).

Since in many bauxite deposits the amount of such larger particles is relatively small it is best to start from larger quantities (0.5-1 kg). Loose types of bauxites are simply disintegrated with water and washed on an 0.06 mm sieve. The residue is repeatedly suspended in water and washed on the sieve.

In the case of harder bauxites that will not readily form suspension in water, freezing or ultrasonic treatment is applied. If this procedure proves effective, the sample is boiled in 10 % HCl for about 0.5 hour. This method usually appears expedient, but has the disadvantage that mineral particles soluble in hydrochloric acid (e.g. apatite) will decompose.

The washed and cleaned particles are subsequently separated into sieve fractions (0.06-0.1 mm, 0.1-0.2 mm and 0.2-0.3 mm).

Each fraction is weighed on an analytical balance and its percentage by weight is calculated. The fractions are then separated into light and heavy fractions, using a highdensity liquid (usually bromoform).

For identification of minerals, the generally known immersion method on the polarizing microscope is applied. The identified mineral particles are counted and a frequency table is composed. This table should be based on a number of identified particles as large as possible. The acceptable minimum is 100 particles. Below this number, statistical distribution is not sufficiently reliable. Vörös, in his micromineralogical study of bauxites from Gánt, identified 1000 particles per sample. (1971)

When the heavy fractions contain many ore particles, the magnetizable ones can be separated by means of magnetic grader. This method is not applicable to very dense and hard bauxites (e.g. Devonian bauxite from the North Ural).

The dominating species in a mineralogical table may be by detrimental mineral particles that got into the bauxite (quartz, rutile, turmaline, garnet, zircon, etc.) as well as larger antigeneous particles of diagenetic or epigenetic origin (pyrite, gypsum, titanohematite, etc.) as in the case of Hungarian bauxites. It should be kept in mind that the results obtained by microscopy apply only to that part of the ore which was separated by the method of preparation, which should be therefore representative.



## OTHER COMPLEMENTARY METHODS

Among other complementary methods one could mention electron paramagnetic resonance (EPR), nuclear magnetic resonance (NMR), neutron diffraction, high temperature diffractometry, Raman spectrometry, photoelectron spectrometry (ESCA), X-ray spectrometry and another "probe" method: ion-probe micro analysis.

These methods seem to be exploited in the studies of rather special problems mainly in the sphere of background research and not in that of technological or practical applications. They are also fairly expensive.

Nevertheless, some very important structural, mineralogical knowledge upon bauxite minerals resulted already from such "complementary" investigations.

For example the position of hydrogen ions and the exact arrangement of hydrogen bridges in aluminiumhydroxides could be determined exclusively by neutron diffraction. The experimental setup at the neutron diffractio measurements is very similar to that of X-ray diffractometry, except the dimensions. A reactor generates the neutrons and since the wavelength of this "radiation" is orders of magnitude larger than that of the X-rays all parts of the apparatus, the required volume of the specimen, etc. are scaled up. Nonetheless the basic equation supporting this technique is the Bragg equation and the methods of interpretation are common with X-ray crystallography. The scattering changes not monotonously with the atomic number and light elements have large scattering factors. This is the reason why hydrogen ions show up well in neutron diffraction studies.

Such work on boehmite was carried out quite recently (Achiwa, Yamamoto and Kawano, 1977) putting an end finally

to a 50 years old dispute concerning the complete structure of this monohydrate mineral by fixing also the location of hydrogens.

Raman spectrometry complements IR absorption measurements. In contrast to the latter one, here monochromatic visible light (produced preferably by a laser source) is used to illuminate the sample, however, the detected absorption effects are interpreted similarly in terms of the vibrational and rotational states of the molecules. Combined application of the two techniques provides more convincing evidences in a much broader frequency range. Additionally Raman spectrometry permits the study of aqueous solutions, too. In case of solids the orientation of bonds can be determined using polarized light.

#### QUANTITATIVE PHASE ANALYSIS OF BAUXITE

General experience have proved that the phase analysis of multicomponent mineral mixtures, like bauxites, can be accomplished with the highest reliability if several methods (polarisation and electron microscopy, X-ray diffraction, IR spectrometry, thermal analysis, etc.) are used in a complementary manner (Bárdossy, 1972). However, it seems to be reasonable to start the mineral phase analysis by X-ray diffraction measurements, because it can detect the widest range of phases, and switch over to an other method only if unresolved problems emerge. Several authors have put forward proposals for the quantitative diffractometric mineral analysis of multicomponent mixtures (Bárdossy, 1966; Moore, 1968; Chung, 1974, 1975; Johnson, 1978). The advent of highly automated X-ray equipment in the recent years has contributed a great deal to the fast and precise measurement of mineral content. Programmed controls for goniometer scanning and integration of counts over selected angular intervals, data processing by computers had reduced considerably the time needed for quantitative analysis. Hence substantial cost savings can accrue from the use of quality control procedures based on automated

quantitative analysis. However, total automation of bauxite analysis have not been achieved yet in the sense of a "sample in - result out" black box. Data acquisition and bookkeeping even in the form of a data bank present causes no problems in this respect, but the programs can hardly cope with the scarcely known crystallographic variability of these minerals and extremely careful monitoring of automatic interpretation is necessary. Thus the use of interactive computer programs is justified.

Diffractometric quantitative phase analysis has a history of 40 years, but recent efforts have been concentrated essentially on the possibilities of avoiding lengthy calibrations and the need of well defined standard samples. Some problems, like preferred orientation and particle size distribution in the specimen, overlapping of the diffraction peaks and their shifts as well as changes in relative intensities due to solid solution effects and mineral individualities, the uncertainties of the intensity conversion factors (ICF-s) etc. render the quantitative phase analysis difficult in most practical cases. Depending on the material system studied, one or more of these difficulties become dominant and others can be neglected.

In bauxites 160 minerals have been identified so far, however, only 20 of them occur in rock-forming quantities. From these latter ones the following minerals are included in the phase library of the program developed in the X-ray laboratory of ALUTERV-FKI (Bárdossy, Bottyán, Gadó, Griger and Sasváry (1979): boehmite, gibbsite, diaspor, corundum, goethite, hematite, pyrite, siderite, kaolinite, chamosite, anatase, rutile, calcite, dolomite, crandallite, lithiophorite and quartz. The problem of the compositional variability generally encountered in the phase analysis of clay rocks is not present in the case of bauxites due to the fact that usually the only clay mineral component is kaolinite with fixed stoichiometry. During the analysis of a huge number of bauxite samples it

turned out that the main sources of uncertainties are here:

- isomorphous substitution, and
- the variation of the intensity conversion factors.

In order to diminish these effects the following procedure has been adopted for computer implementation:

It is assumed that the set of minerals included in the phase library covers all the components present in the samples and a complete identification is possible.

After the determination of the extent of isomorphous substitution from peak shifts the correct stoichiometry of all phases is regarded as known.

Consequently a matrix can be defined

$$Q(i,j) = S(i,j) \cdot r(i,j) \cdot s(i)^{-1}$$

with elements characterizing the contribution of the j-th chemical constituent (oxide, radical, etc.) to the i-th phase ( $0 \leq Q(i,j) \leq 1$ ).

Where

- $s(i)$  - is the molar weight of the i-th phase,
- $S(i,j)$  - is the molar weight of the j-th chemical constituent occurring in the i-th phase,
- $r(i,j)$  - is a coefficient related to the thermal decomposition of the i-th phase.

The actual chemical composition of the sample can be determined up to 98-99 % by analysis for a definite number (J) of elements. Chemical analysis can be also automated if accomplished by atomic absorption spectrometry (AAS) or X-ray fluorescence analysis (XFA). The phase analysis will be consistent with the elemental analysis if the equation

$$\sum_{n=1}^H x(n) \cdot Q(n,j) = e(j) \quad (4.1)$$

is satisfied, where

- $e(j)$  - is the analysed quantity of the  $j$ -th chemical element,
- $x(n)$  - represents the weight percentage of the  $n$ -th component in the mixture,
- $H$  - is the number of identified phases.

Equation (4.1) will be eo ipso satisfied if the phase percentages are calculated from the measured diffracted intensities and the chemical analysis data using the equation

$$x(i) = T(i) \cdot e(1) / \left[ Q(i,1) \cdot \sum_{n=1}^H T(n) \right], \text{ where (4.2)}$$

$$T(i) = C(i,1) \cdot I(i), \text{ and (4.3)}$$

- $C(i,1)$  - the relative intensity conversion factor (RICF), referring to the  $1$ -th chemical constituent,
- $I(i)$  - weighted average intensity of the  $i$ -th phase calculated from several measured integrated peak intensities.

Remarkable is the use of  $C(i,1)$ -s in Eq.(4.2) through Eq. (4.3) permitting the conversion of measured intensities to phase percentages within a group of phases containing the

same chemical constituent (e.g. gibbsite, diaspore, boehmite and corundum containing all aluminium). Within each such group (1) one RICF can be set equal to unity by choosing the relevant phase arbitrarily as a reference for the very group. Subdividing the phases being analysed into as many groups as the number of main chemical elements, errors due to the uncertainties of the ICF-es are not carried over to the next subgroup and each group is normalised in itself by an elemental analysis.

The self-consistency of the mineral phase analysis accomplished by the proposed method can be checked through three calculated figures:

1. The sum of the calculated phase percentages should be  $\sim 99\%$ . Undetected material is deemed to be acceptable up to 1%, however, higher deficiencies give rise to suspicions concerning serious faults in the identification or the presence of significant amorphous content.

2. The total calculated loss on ignition (LOI) should match the measured LOI (determined in air in the temperature range 105-1300 C degree) 1).

3. The calculated effective ICF-s for each phase should fall into the range determined empirically for the main bauxite components (Bárdossy & al. 1977).

Diffracted X-ray intensities are collected on punched tapes by a Philips diffractometer equipped with automatic sample changer. The measurements are made in the  $2\theta$  range  $5-55^\circ$  with  $0.05^\circ$  sampling. The data processing is carried out on a 16K byte Hewlett-Packard desk calculator programmable in BASIC language.

The measured intensity data of a set of 38 diffraction patterns can be stored on cassettes. The files allocated to the pattern contain all the data necessary to identify the samples and the conditions of the measurement. These files accommodate as well the quantities derived in the course of the calculations.

The data processing is completely automatic. The baseline is determined in three consecutive steps:

- a) the measured counts are gathered into groups of tens and then the average value within each subgroup is assigned to the first point,
- b) a set of averages monotonously decreasing with the scattering angle is selected,
- c) the final baseline is fitted to those points of this set which can be connected by straight lines with monotonously decreasing slopes.

The intensities are then corrected for the background scattering. The data are smoothed, the location, amplitude and integrated intensity of each peak is determined by a procedure in which the following conditions must be fulfilled for a peak position:

- (i)  $I(i-1) < I(i) > I(i+1)$
- (ii) either three monotonously decreasing counts follow  $I(i)$  in both directions, or there are at least four monotonously decreasing counts in one direction, and
- (iii) the peak localized this way is statistically significant i.e.  $I(i) > 3 \cdot \sqrt{B(i)}$ , where  $I(i)$  is the measured count in the  $i$ -th point of sampling and  $B(i)$  is the corresponding background count.

Integrated intensities are calculated for single peaks by summarizing the counts from background to background in both directions, where the observed count is regarded as background

if  $I(i) < 3 \cdot \sqrt{B(i)}$ . Overlapping peaks are separated at the local minimum points.

The interpretation and correction of the patterns are carried out in an interactive mode. The processed diffractogram is drawn by the X-Y plotter on a preprinted form containing some information useful for the evaluation of bauxite patterns. This includes bars positioned on the  $2\theta$  scale corresponding to the most important reflections of bauxite mineral marks label the reflections calibrated for isomorphous substitutions (33 %) as well as the reference lines (\*) (Fig.4.31).

The user definable keys of the calculator are programmed to permit the operator a wide variety of easy corrections (recalibration of the  $2\theta$  scale, deleting parasitic peaks, defining new ones, reintegration of the peaks, etc.)

Next the calculator searches for the phases present and comes up with a printed proposal of preliminary identification. Once the preliminary qualitative analysis has been accepted by the operator, the program looks for a complete matching between the observed reflections and the data of the phase library.

In the last subroutine the phase percentages are computed in four steps:

1. The  $Q(i,j)$  matrix of Eq.4.1 is modified according to the substitutions determined from the peak shifts (calibration curve e.g. for goethite can be seen in Fig.4.32, the others for hematite, diaspore, calcite, etc, are similar).

2. Input of the chemical analysis data. It is appropriate to analyse bauxites for Al, Fe, Si, Ti, Ca, Mg, S, P, Mn, C and the loss on ignition. Because of the interference of certain peaks it is recomandable is some cases to determine chemically the non-reactive silica, too, which can be taken as quartz. Similarly it can be very useful to know separately the re-



ALUTERY - FKI  
 X-RAY LABORATORY  
 BAUXITE  
 DIFFRACTION  
 CU K-ALPHA RBD 4KV 20MA  
 SPECTRUM PLS COUNT TIME: 1250  
 MAXIMUM COUNT: 11225  
 CHART NO: 1129  
 SAMPLE: FEUERHEBE

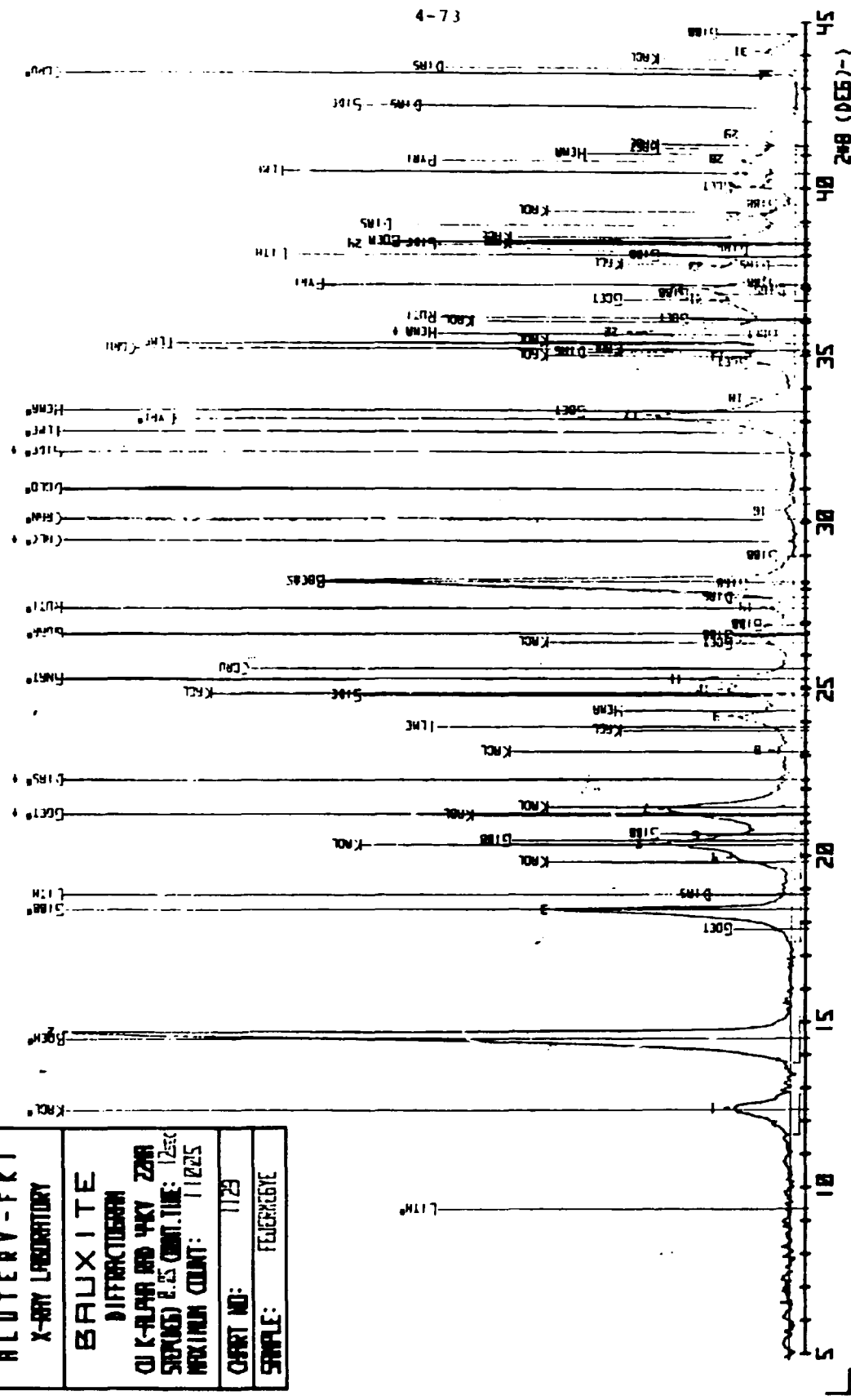


Fig. 4.31  
COMPUTER PROCESSED DIFFRACTOGRAM OF A BAUXITE SAMPLE

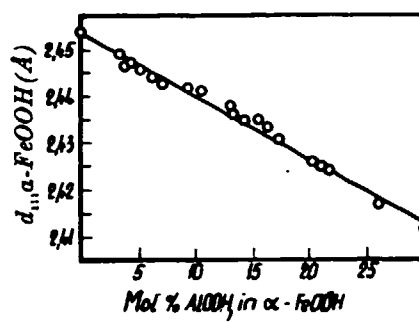


Fig. 4.32

THE  $d_{111}$  LATTICE PARAMETER OF GOETHITE AS A  
FUNCTION OF Fe/Al SUBSTITUTION

spective amounts of bivalent and trivalent iron ions.

If a chemical analysis is not available the program proceeds using the ICF-s from the library and a

$\sum x(i) = 100$  % normalisation. In this case step 3. is omitted, but consequently larger errors are likely.

3. The calculation of phase percentages starts with the column of the  $Q(i,j)$  matrix containing least non-zero terms. The quantity of this element is distributed among the relevant phases according to Eq.4.2 in order to yield the percentages of mineral components. On the other hand the amounts of other elements required stoichiometrically for the phases already fixed are subtracted from the terms of the remaining columns. This procedure is repeated until all chemical constituents are handled in turn. The LOI is not tackled but used for control together with the sum of phase percentages and the calculated ICFS, which are all derived in this step.

4. The final table of results is printed, a sample of which can be seen on Fig.4.33.

Complementary diffraction patterns are taken for accurate determinations in the following cases:

- (i) If the clay mineral is not kaolinite, the sample is treated with glycerine or ethylene glycol to see whether this treatment leads to a shift of the basic reflection.

This eventual shift is also studied on a sample heated to 500 °C. The patterns are interpreted by means of the internationally established keys for clay mineral identification.

- (ii) The higher the iron content in the bauxite, the higher the average mass absorption coefficient and hence the limit of detection for individual minerals. For this reason, bauxite samples with  $Fe_2O_3$  percentages

ALUTERV-FKI X-RAY LABORATORY  
 BUDAPEST, 5.03.79.

SAMPLE: FEJERMEGYE

RECORD NO.: 1129

HEMATITE: 2.6 m%  $Al_2O_3$                       d(110) = 2.512              d(110)st = 2.515 A  
 GOETHITE: 22.7 m%  $AlOOH$                       d(110) = 4.152              d(110)st = 4.200 A

	$Al_2O_3$ %	$Fe_2O_3$ %	$SiO_2$ %	$TiO_2$ %	LOI %	Integr.i	PHASE %	ICF	REL.DEV.	RICF
HEMATITE	0.14	7.86				19972	8.0	0.90	-0.7	1.00
BOEHMITE	27.56				4.86	72538	32.4	1.00	-0.0	1.00
GOETHITE	1.86	9.94			1.45	21045	13.3	1.41	-1.4	1.20
GIBBSITE	11.29				5.97	22866	17.3	1.69	2.4	1.30
KAOLINITE	9.51		11.20		3.37	10203	24.1	5.29	-0.1	5.40
ANATASE				2.16		9872	2.2	0.49	1.9	0.80
RUTILE				0.64		2351	0.6	0.61	2.1	1.00
CRANDALL	0.45				0.18	587	1.3	5.14	0.1	2.00
ADS. $H_2O$					0.36		0.4	BOEHMITE REF.		
CAL. COMP.	50.81	17.80	11.20	2.80	16.19		99.6			
ANALYSIS	50.80	17.80	11.20	2.80	16.20		98.8			

4-76

Fig. 4.33  
 THE FINAL TABLE OF RESULTS IS PRINTED, A SAMPLE OF WHICH  
 CAN BE SEEN ON FIG. 4.33

exceeding 15 % are heated in boiling 10 % HCl for 5 to 15 minutes. We do not aim at a complete dissolution of the iron minerals, but only at the dissolution of their major part. Then a diffraction pattern is again taken. Here, owing, to the reduced mass absorption coefficient, minerals will be revealed which in the first diffraction pattern did not reach the limit of detection (this is particularly important in the case of kaolinite and other clay minerals). On the other hand, peaks that are covered in the first diffraction pattern by the reflections of iron minerals also become identifiable.

- (iii) In gibbsitic bauxites, quartz in the order of 0.1 % cannot be detected, owing to the interfering effect of gibbsite reflections with the two most intensive quartz reflections (100-intensity at 3.343 Å and 19-intensity at 4.254 Å). In such cases we heat the sample for one hour at 350 °C. As a result, gibbsite will decompose, its reflections will disappear and quartz reflections become measurable in the new diffraction pattern.
- (iv) In bauxitic clays, with kaolinite content exceeding 50 %, the 100-intensity kaolinite reflection at 3.573 Å usually totally conceals the strongest anatase reflection at 3.51 Å. To identify anatase unequivocally, the sample is heated for one hour at 550 °C and a new diffraction pattern is made. In this pattern, the hitherto covered anatase reflections appear, since kaolinite is decomposed in the course of the heat treatment.

Recourse to thermal analysis is made first of all to check or complete the results upon aluminium bearing minerals. On the basis of an example the thermal procedure will be discussed for a bauxite sample containing gibbsite, boehmite, diaspor, kaolinite, quartz and alumogothite. The DTG and TG curves of this bauxite and of three red muds obtained by digesting at three different temperatures are presented on Fig.4.34. No DTA curves are presented since for this actual case they offered no additional information and the selectivity

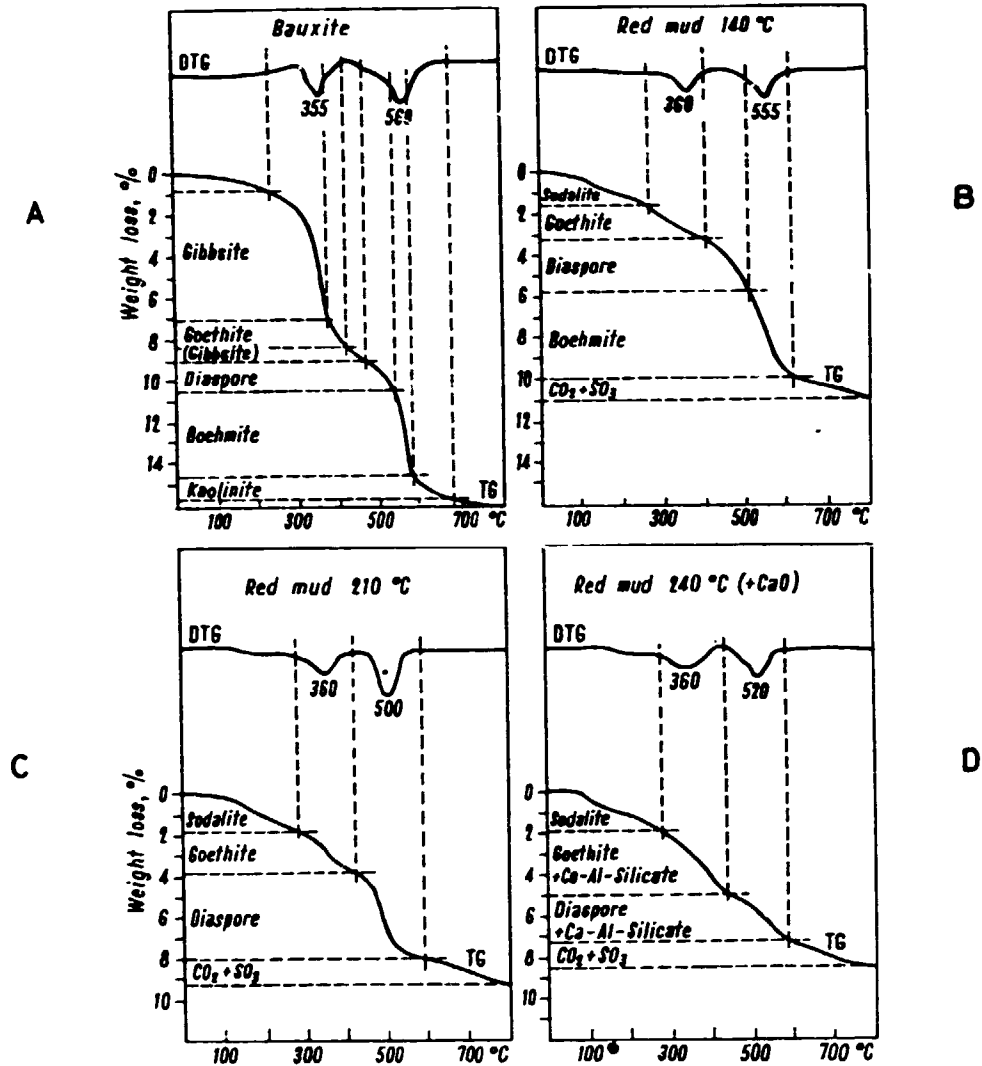


Fig. 4.34

DTG AND TG CURVES OF A MIXED BAUXITE AND  
OF RED MUDS OBTAINED THREE DIFFERENT  
DIGESTION TEMPERATURES

of the DTG curves proved to be better.

Identification of the constituents was not unequivocal in the bauxite derivatogram (A). As a result of digestion at 140 °C for 1 hour (B) gibbsite was removed and the kaolinite converted into sodium aluminium hydroxalicate. One hour digestion at 210 °C resulted in the dissolution of boehmite. Finally by adding 4 % CaO and digesting for 1 h at 240 °C diasporite was partially dissolved (D).

The procedure for calculating the mineralogic composition starts with the evaluation of Fig.4.34-C. From this the diasporite content is calculated. This value is then used to determine the diasporite content of samples B and C, based on their Al<sub>2</sub>O<sub>3</sub> content. Subsequently the boehmite percentage is determined for B. The boehmite and diasporite content now being known, the kaolinite content in sample A (i.e. the initial bauxite) can be calculated. The alumogothite percentage and the composition of this mineral can be calculated in samples B and C. From these data the alumogothite and gibbsite content of the bauxite is calculated. Finally the mineralogic composition of the bauxite is found to be:

6.4 % weight loss	Gibbsite	13.2 % Al <sub>2</sub> O <sub>3</sub>	
1.4 % weight loss	Alumogothite	1.1 % Al <sub>2</sub> O <sub>3</sub>	8.9 % Fe <sub>2</sub> O <sub>3</sub>
2.35 % weight loss	Diasporite	13.3 % Al <sub>2</sub> O <sub>3</sub>	
3.25 % weight loss	Boehmite	18.4 % Al <sub>2</sub> O <sub>3</sub>	
1.1 % weight loss	Kaolinite	3.1 % Al <sub>2</sub> O <sub>3</sub>	3.6 % SiO <sub>2</sub>

The limit of detectability is somewhat lower in diffractometry than in the thermal analysis for almost all bauxite minerals. However, amorphous organic matters cannot be detected by X-rays, while the derivatograph reveals its presence even in concentrations as low as 0.1 % C<sub>org</sub>. Similarly, absorbed water the amount of which is usually 0.2-2.0 % in bauxites, can be measured only by thermal methods. The higher, the

percentage of absorbed water is the more porous and fine grained the bauxite will be. On the other hand, it can be duely suspected that such water is mainly absorbed by iron and manganese minerals, because samples treated with hydrochloric acid indicated lower percentages of absorbed water than the original ones.

IR absorption spectrometry has also its own merits in a quantitative phase analysis. It has to be mentioned that very small (2.5-3.0 mg) quantities of material are sufficient for a KBr pellet sample thereby permitting the separate study of smaller textural elements. The verification of the extent of isomorphous substitution determined by diffractometry can be accomplished, too. Further to the case of alumogoethite also ferridiaspore and ferriboehmite can be checked.

Experiments performed with the aim to determine the limit of detectability of gibbsite, boehmite, kaolinite, diaspore and goethite gave the following data:

mineral	limit of detectability by IR absorption spectrometry, %
gibbsite	3-4
boehmite	2-3
diaspore	> 10
goethite	> 10
kaolinite	2.5 in boehmitic bauxites 3,5-4 in gibbsitic bauxites 5 in diasporic bauxites



Finally the limit of detectability can be reduced below 2.0 % for all bauxite components and is around 0.3 % for the most important ones if the recommended complex method, selective dissolutions and complementary techniques are exploited:

Mineral	Limit of detection	
	using the basic methods, %	also making use of complementary methods, %
Illite	2.5	2.0
Chlorite	2.2	1.8
Halloysite	2.0	1.5
Kaolinite	1.5	1.0
Chamosite	1.2	1.0
Corundum	0.5	0.3
Diaspore	0.5	0.3
Gibbsite	0.5	0.4
Boehmite	0.5	0.3
Maghemite	0.4	0.3
Marcasite	0.4	0.1
Pyrite	0.3	0.1
Magnetite	0.3	0.1
Hematite	0.3	0.2
Goethite	0.3	0.2
Siderite	0.2	0.2
Dolomite	0.2	0.1
Calcite	0.2	0.1
Quartz	0.2	0.1
Rutile	0.1	0.05
Anatase	0.1	0.05
Zircon		0.05

The error of the analysis is about  $\pm 2$  % rel.

A solid is referred to as heterotypic if its different physical, chemical or structural parameters can not be specified by a single numerical value but as spread out in a more or less wide range with some kind of characteristic distribution. In order to describe samples correctly it is thus necessary:

- a) to define exactly the parameter used for this purpose; (One can choose primary measures like particle size, chemical composition, lattice dimensions, etc. or secondary (derived) ones like IR absorption frequencies, the widths of X-ray reflections, etc.),
- b) to give the average value of the chosen parameter, and
- c) the distribution of measured values around this average.

Heterotypism is an almost inevitable, general feature of solids. Homotypism occurs in nature very scarcely and can be achieved in synthetic materials only by extremely careful control of the preparation.

We are talking about the individualism of a sample regarded as uniform because it had been collected at a certain site or prepared in a well defined manner if its studied parameter exhibits a different average value or a different distribution around the average than a reference sample of the same solid species.

From the above definitions it is clear that the recognition as well as the distinction of heterotypism and individualism depend partly on points of views partly upon the accuracy and resolving power of the instruments used for the investigation of solids.

If a sample is regarded as integral entity it might be possible to study its heterotypism provided we dispose with

methods delicate and reliable enough to determine the distribution of any parameter or to reveal minor differences existing between the parameters measured in various fractions of the very sample.

If certain samples are separated from each other, similarly accurate analyses can prove their individualism. As the experimental technique of scientific research develops individualism is specified more and more frequently and precisely. E.g. the structural variability of boehmite samples could not be detected by measurement of the diffracted integral intensities, however, the more advanced pattern-fitting structure refinement seemed to be successful in this respect.

As already pointed out during the discussion of the most frequently used methods of mineralogical bauxite analysis, i.e. X-ray diffractometry, thermal analysis and IR spectrometry, the calibration parameters are dependent on this individualism or in other words on the origin of the sample. These "mineralogical errors" give more frequently than not the dominant uncertainties before the instrumental or methodic errors.

Bárdossy and his co-workers (1977) published data concerning the range of intensity conversion factors (ICF) to be used in X-ray diffractometry:

Mineral	range of ICF
boehmite	1*
gibbsite	0.5 - 1.2
diaspore	0.9 - 1.2
kaolinite	1.4 - 8.0
hematite	0.5 - 4.6
goethite	0.8 - 4.5
anatase	0.3 - 0.7

\* arbitrarily selected reference

It should be noted that the individualism of some minerals has a very prominent influence on the ICF, e.g. for kaolinite the ratio might be 1:5, for hematite 1:9 and for goethite 1:6. Thus mineralogic quantitative phase analysis based on ICF-s can be accurate only if these are determined specifically for each deposit. This is done either by means of standard minerals from the region in question, or if such samples are not at disposal, by comparing the X-ray results with complete chemical analysis and derivatograms, IR results or any other independent evidences and performing corrections in order to gain self-consistent results. If long suites of samples are analysed in this way the mean value of the ICF-s can be established accurately enough to be applied in subsequent measurements of samples from the very deposit.

Similar phenomena appear in IR absorption spectrometry and this fact led Jónás and Solymár (1970) to the introduction of the "relative intensities" which are less sensitive to individualism.

Rather substantial heterotypism is exhibited by the X-ray half-width of boehmite samples as demonstrated on Fig.4.35. Heterotypism is represented here by the fact that the plotted parameters are not constant for the separated fractions. Individualism results in different curves for the samples from various locations.

Another interesting example of significant mineral variability is shown in Fig.4.36, where the shape of the X-ray reflection of some goethites is represented.

Everything mentioned above has serious consequences for the research and development activity aiming at the improvement of the phase analysis. This sets as a crucial task the study of real structures, the elucidation of relationships existing between some well measurable parameters and the

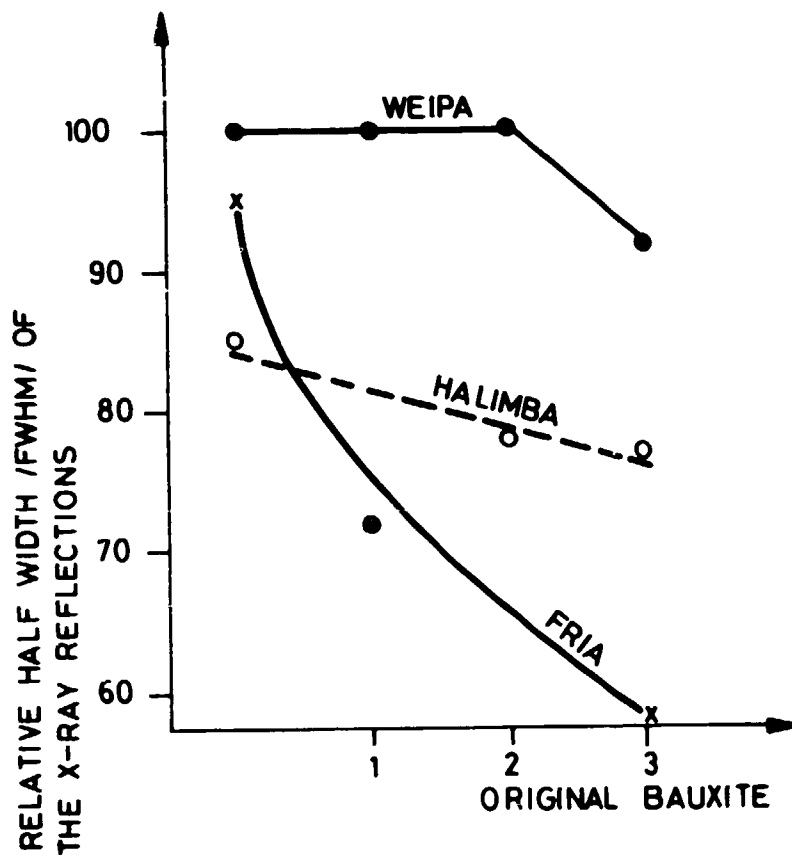


Fig.4.35

THE RELATIVE BREADTH OF THE 020 X-RAY REFLECTION FROM THREE BAUXITES. THE ORIGINAL BAUXITES AND SOME FRACTIONS WERE MEASURED AS MARKED ON THE HORIZONTAL AXIS

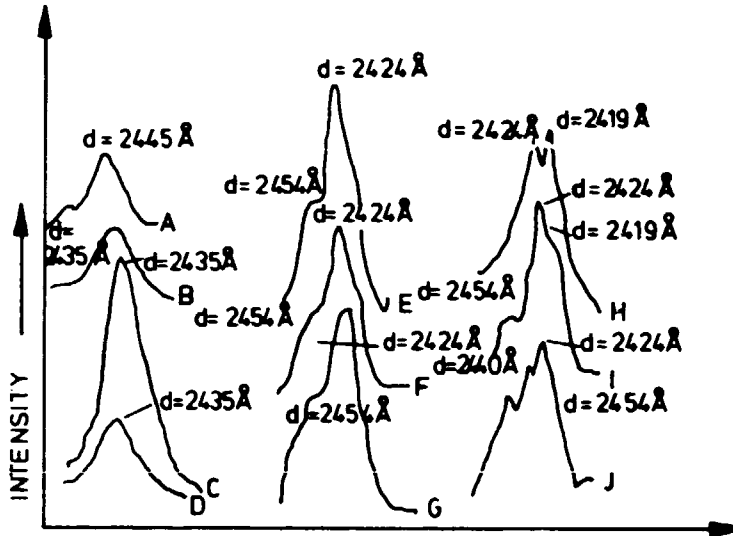


Fig. 4. 36

X-RAY DIFFRACTION TRACES OF GOETHITE IN BAUXITE  
/A - D/ AND MUDS /E - J/ SHOWING VARIATIONS IN  
ALUMINIUM SUBSTITUTION

conversion factors used in almost all analytical methods. The ideal state would be if correlation could be found between well measurable features and the actual values of the calibration parameters. Such trial is in the field of X-ray diffractometry to use the  $I_{1\bar{1}0} / I_{1\bar{1}1}$  intensity ratio to select the appropriate ICF for kaolinite.

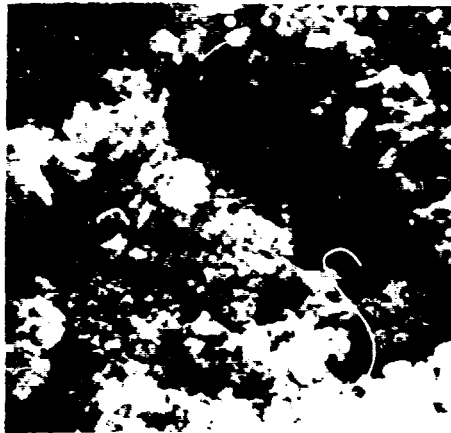
A systematic work has been started to determine the structural variability of boehmite (Farkas, Gadó and Werner, 1977). Using several accurate methods it was proved for 15 samples from widely dispersed locations that the ICF of boehmite does not change significantly (despite the fact that there are some definite changes in the structural parameters). Therefore it seems to be justified to set  $ICF_{boe} = 1$  as a reference in the bauxite phase analysis.

### 3. MINERALOGICAL INVESTIGATION OF RED MUD

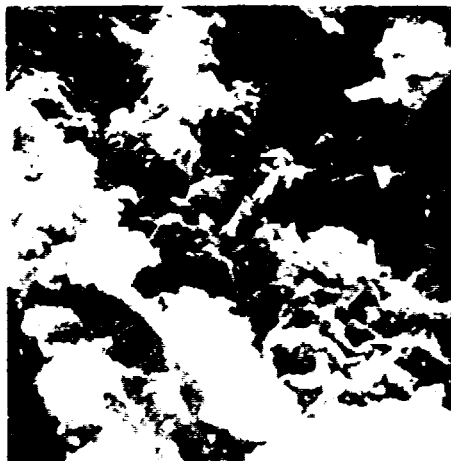
Since the basic mineralogical methods applied to red muds are identical with those described in respect of bauxites only the special features characteristic for red muds will be emphasized in this section.

Fig.4.37 shows typical scanning electronmicroscopic images of a red mud and its components.

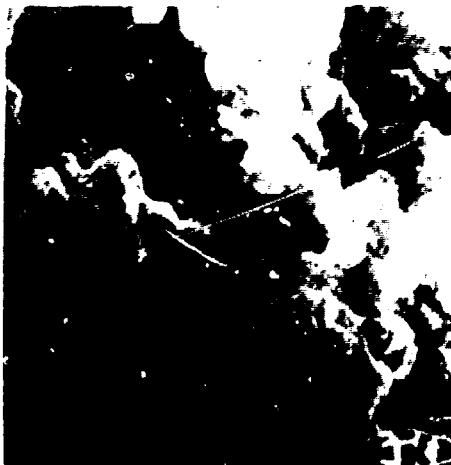
From the technological point of view the determination of all components of red mud is essential. However, measurement of the aluminium containing phases is of greatest importance. These phases include:



A.  
RED MUD 300°



B.  
CANCRINITE



C.  
CO<sub>3</sub>-SODALITE  
10000 X

Fig. 4.37  
SCANNING MICROGRAMS OF A RED MUD /A/ AND  
TWO OF ITS SIGNIFICANT COMPONENTS:  
CANCRINITE /B/ AND CO<sub>3</sub> SODALITE /C/



- a) the group of aluminium minerals left undigested, e.g. boehmite diaspore and partially substituted iron oxides,
- b) the phases formed in the reaction of silica with aluminate liquor, i.e. sodalites and cancrinites,
- c) gibbsite formed by hydrolysis of the red mud,
- d) calcium aluminium silicates formed corresponding to equilibrium conditions in the presence of lime.

The measurement of residual boehmite in the red mud is a suitable tool for checking the operation of the digesters. On the other hand if digestion is carried out under strictly defined conditions, the amount of boehmite in the red mud may serve as a measure of crystallinity, or may indicate stability of structure due to other causes, e.g. foreign ion doping.

The determination of diaspore and alumocompounds like alumogoethite, alumohematite and alumomaghemite allows to calculate the difference between theoretical and practical yields.

The measurement of alumina in sodium aluminium hydro-silicates permits to determine the combined and inevitable losses.

Determination of calcium aluminates allows to fix optimum amounts of CaO to be added during digestion.

Besides aluminium containing phases of primary importance, the determination of iron minerals - goethite, hematite, maghemite - should not be neglected, since aluminium incorporated in these minerals can be calculated exactly only if their percentages are known. On the other hand, the goethite and hematite contents and their ratio yield valuable information on settling properties.

Three methods are being used currently for phase analysis of red muds: X-ray diffraction, derivatography and IR spectrometry.

All three methods are suitable for determining the phase composition of red muds. However, if only a single method is to be applied, X-ray diffraction is doubtlessly the one that yields most information, since it allows fastest detection of the largest number of constituents and - with the exception of one or two phases - the limit of detectability is for this method the lowest.

The absolute values are less defined when IR spectrography is applied., since excitation greatly depends on the degree of crystallinity. Also, the percentage and nature of foreign ions incorporated by isomorphous substitution substantially affect extinction. However, for the very reason that band width depends on crystallinity to a large extent, IR spectrometry, though less suited for exact quantitative determinations. yields highly valuable information in cases when red muds obtained in the same technological process from bauxites of different origin are being compared.

Percentages can also be determined by derivatography. It must be admitted that this method is more influenced by the phase composition than diffractometry, since the values are liable to become less distinct owing to superpositions of the peaks.

Nonetheless, certain phases will be particularly well determined by one or the other method. Thus, gibbsite is detectable by IR spectrography even when present in traces only. Similarly, IR spectrometry permits to determine kaolinite in the solid material slurries desilicated before digestion in percentages as low as 1 %. This fact is of great importance, because X-ray diffraction allows to determine kaolinite only

when its quantity exceeds 2 %, whereas if desilication of the slurry is satisfactory, the resulting red mud will contain only 1-2 % kaolinite. Also kaolinite often exhibits flat, broad reflections, while its IR bands are always very intensive, independently of the crystallinity of the other phases.

Derivatography is particularly suited for determining absorbed and combined water as well as gibbsite formed by hydrolysis of the red muds. In addition derivatography has the advantage that it is suitable for the determination of amorphous phases and that the shift of peaks indicating water release offers information concerning the stability of the internal structure.

Thus the three methods effectively complement each other.

#### X-RAY DIFFRACTOMETRY

Qualitative identification of the crystalline phases are being carried out using the PDF cards. If coincidences occur the relative intensities and reflections free from interferences should be taken into account in course of the interpretation.

The mineral components of red muds can be classified in the following manner:

- a) minerals deriving from the parent bauxite:
  - unchanged aluminium-oxy-hydroxides (boehmite and diaspore)
  - iron minerals (hematite, goethite, lepidocrocite, limonite)
  - unaltered accessory phases (rutile, anatase, pyrite, calcite, dolomite)

b) phases formed in course of the Bayer process:

- hydroxy sodalites
- titanium oxy-hydrate gel
- $\text{NaHTiO}_3$
- gibbsite

c) phases produced during the caustisation of red mud

- calcium aluminium hydrosilicates
- tricalcium aluminate
- $\text{Ca(OH)}$  residue

The following data are used for the identification of the most frequently occurring phases:

Component	d (Å) value of the diagnostic reflection	FDF card number
Gibbsite	4.83	12-460
Boehmite	6.11	21-1307
Diaspore	3.98	2-0355
Quartz	3.34	5-0490
Dolomite	2.88	11-78
Calcite	3.04	5-0586
Anatase	3.51	21-1272
Rutile	3.25	21-1276
Goethite	4.17	17-536
Alumogoethite	2.45	17-536
Hematite	2.69	13-534
Alumohematite	2.51	13-534
Maghemite	2.51	25-1402
Sodalites	6.30 - 6.38	20-1070
Cancrinites	4.61 - 4.70	20-257
Calcium aluminate ( $3 \text{CaO} \cdot \text{Al}_2\text{O}_3 \cdot 6 \text{H}_2\text{O}$ )	5.16	3-0125
Calcium titanate ( $\text{CaO} \cdot \text{TiO}_2$ )	1.91	9.365

For sodalites and cancrinites a range of  $d$  values has been published since the nature of salt impurities and anion concentration in the digesting liquor, as well as digesting temperature and the molar ratio of the digesting slurry have a great effect on the nature of the sodalite and cancrinite formed, namely whether the product will be hydroxide, chloride, carbonate or aluminium sodalite, normal or basic cancrinite, respectively. All these factors will influence the  $d$  value at which the reflection of the mixed crystal will appear. In addition,  $d$  values for sodalites and cancrinites may also change owing to structural reasons. The channel like structure characterizing these phases allows the incorporation of foreign ions, which in turn results in a shift of the  $d$  values. Shifts due to such causes or to isomorphous substitution have not been listed, since the extent of the shift is always a function of the degree of substitution. Note that this phenomenon can be substantial also in the case of  $3 \text{CaO} \cdot \text{Al}_2\text{O}_3 \cdot 6\text{H}_2\text{O}$  and  $\text{CaTiO}_3$ .

The following observations and experimentally established facts can serve as a basis aiming the phase analysis of red muds:

(I) In order to control the efficiency of certain technological operations, e.g. digestion, the knowledge of the complete phase composition of red mud is not always necessary. The determination of e.g. boehmite or gibbsite, or some other single phase may be satisfactory. Therefore a method is required permitting the determination of any constituent in itself, too.

(II) The decisive factor affecting the crystallinity of the phases of red mud is not crystallinity of the bauxite, but the conditions under which the red mud was produced, first of all the temperature at which digestion was carried out.

(III) Changes in crystallinity will manifest themselves in changes of peak heights and areas, resp. of the reflections. To eliminate this factor it is indispensable to use a

crystallinity reference. We found hematite best suited for this purpose, partly, because it always appears in a well crystallized form, and partly, because it is the only phase present in large amounts which does not react with aluminate liquor. In the case of red mud, aluminium minerals are unsuitable for this purpose.

(IV) Changes in digestion temperature affect the crystallinity factor of all individual phases of the material to the same extent, even if some of the phases undergo quantitative changes in the course of digestion. For example, much more cancrinite than sodalite is formed in a digestion at 260 °C, while in a digestion at 200 °C the proportions - providing identical conditions and excluding the possibility of CaO excess - will be shifted towards sodalite. However, crystallinity of both cancrinite and sodalite formed at 260 °C is substantially and to the same extent higher for both minerals, than when formed at 200 °C. A similar change has been observed in the proportion of goethite to hematite as a function of digestion temperature.

(V) Findings of other research works connected with the formation conditions, appearance and structure of sodium aluminium silicates can also be utilized. Such findings were: at 180 °C only sodalite, at 230 °C sodalite and cancrinite, at higher temperatures (240 or 260 °C) cancrinite or - depending on the molar ratio of the liquor - cancrinite and sodalite are formed. Alumina to silica ratio in cancrinite was always found to be 1:2, i.e. no excess  $\text{Al}_2\text{O}_3$  was incorporated. For sodalite, this ratio was 1.09 to 1.10. Based on these ratios the determination of one of the constituents combined in sodalite or cancrinite - preferably  $\text{Al}_2\text{O}_3$  - allows the calculation of  $\text{SiO}_2$  percentage. Sodalites formed under the conditions of the Bayer cycle can be characterized by the overall formula  $3(\text{Na}_2\text{O} \cdot \text{Al}_2\text{O}_3 \cdot 2\text{SiO}_2)\text{Na}_2\text{X} \cdot n\text{aq}$ , where X is  $\text{CO}_3^{2-}$ ,  $\text{SO}_4^{2-}$ ,  $2\text{Cl}^-$ ,  $2\text{AlO}_2^-$ ,  $2\text{OH}^-$ , or a mixture of these anions, corresponding to actual concentration and temperature conditions. Normal and basic cancrinite is also characterized by this overall formula,

where X is  $\text{CO}_3^{2-}$  or  $2\text{OH}^-$ .

When technology is stable, the proportion of the listed anions, and consequently the composition of the sodalites formed, remains practically unchanged. If the salt level changes, the reflections will shift owing to changing composition, but no changes will be observable in their heights. If the silica content in the bauxite increases (but remains identical in type) and the salt level remains unchanged, the composition of sodalites and cancrinites will remain unchanged, but their percentage will change.

Based on these experimental findings, the sodalite and cancrinite content of red muds can be characterized by the alumina content, independently of the anions(s) taking part in their formation.

#### THERMAL METHODS

Thermal data for minerals which are common components of bauxites and red muds and have been discussed already will not be repeated here. Diagnostic data for some typical red mud components are given below:

Phase	Formula	Component lost	Peak temp.	Temp. range
Sodalite	$1, 3\text{Na}_2\text{O} \cdot \text{Al}_2\text{O}_3 \cdot 1, 7\text{SiO}_2$ $1, 7 \text{H}_2\text{O}$	$1, 7 \text{H}_2\text{O}$	-	100-400
Ca-Al-Silicate hydrate	$3\text{CaO} \cdot \text{Al}_2\text{O}_3 \cdot 2\text{SiO}_2$ $4 \text{H}_2\text{O}$	$4 \text{H}_2\text{O}$	360-380	280-440
Ca-Al-Silicate hydrate	$3\text{CaO} \cdot \text{Al}_2\text{O}_3 \cdot 2\text{SiO}_2$ $2 \text{H}_2\text{O}$	$2 \text{H}_2\text{O}$	360-380	280-440
Calcium hydroxide	$\text{Ca}(\text{OH})_2$	$\text{H}_2\text{O}$	520	470-550
Calcium aluminate	$3\text{CaO} \cdot \text{Al}_2\text{O}_3 \cdot 6\text{H}_2\text{O}$	$4 \text{H}_2\text{O}$	350	280-420

Results of derivatographic studies upon sodium- and calcium-aluminium silicates can be summarized as follows:

The sodium aluminium silicates formed in course of the Bayer process exhibit sodalite structure with an 0.896 nm unit cell. Due to the presence of carbonate, sulphate and chloride compounds in high concentrations - as already stated - the overall formula of the sodalites can be written as  $3(\text{Na}_2\text{O} \cdot \text{Al}_2\text{O}_3 \cdot 2\text{SiO}_2) \text{NaX} \cdot n\text{H}_2\text{O}$  where X may be  $\text{CO}_3^{2-}$ ,  $\text{SO}_4^{2-}$ ,  $2\text{Cl}^-$ ,  $2\text{OH}^-$  or a mixture of these anions. When the digestion is performed at 210-240 °C the calculations are recommended to be carried out actually using the formula:

$(1.0-1.3)\text{Na}_2\text{O} \cdot \text{Al}_2\text{O}_3 \cdot 1.7\text{SiO}_2 \cdot 1.7\text{H}_2\text{O}$ . Fig. 4.38 shows derivatograms of sodalite and carbonate sodalite produced by the digestion of kaolinite. It may be seen that the water loss is 10 % in the temperature interval 100-400 °C and the exothermal reaction characteristic for the formation of nepheline may be observed, too.  $\text{CO}_2$  escapes at 800 °C. CaO transforms the sodalite during caustization to calcium aluminium hydrosilicates possessing the formula  $3\text{CaO} \cdot \text{Al}_2\text{O}_3 \cdot (1-2)\text{SiO}_2 \cdot (2-4)\text{H}_2\text{O}$ . Tricalcium aluminate losses 4 mole water at 320 °C. peak temperature and 2 mole water at 520 °C, while the hydrosilicate of the above formula dehydrates at 320 °C. Water loss of non-reacted  $\text{Ca}(\text{OH})_2$  being present in excess occurs at 520 °C. Titanium oxyhydrate produced by the digestion of anatase and metatitanate precipitation lose their zeolitic water of about 12 % between 100 and 300 °C. Being aware of these relationships it is possible to determine by means of derivatography the approximate quantities of both sodium aluminium silicate and calcium aluminium silicate as well as the efficiency of caustization.



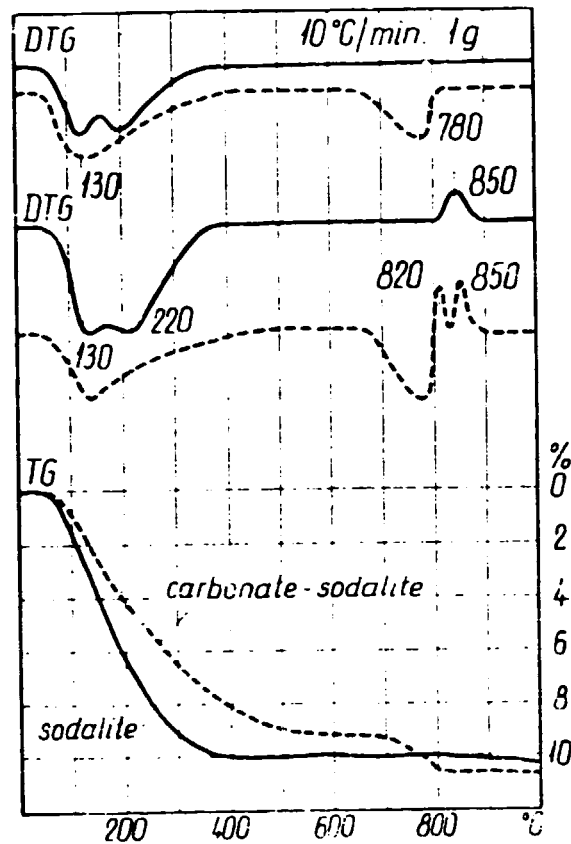


Fig. 4.38

THE DERIVATOGRAM OF SODALITE AND CARBONATE SODALITE, IMPORTANT COMPONENTS OF RED MUD

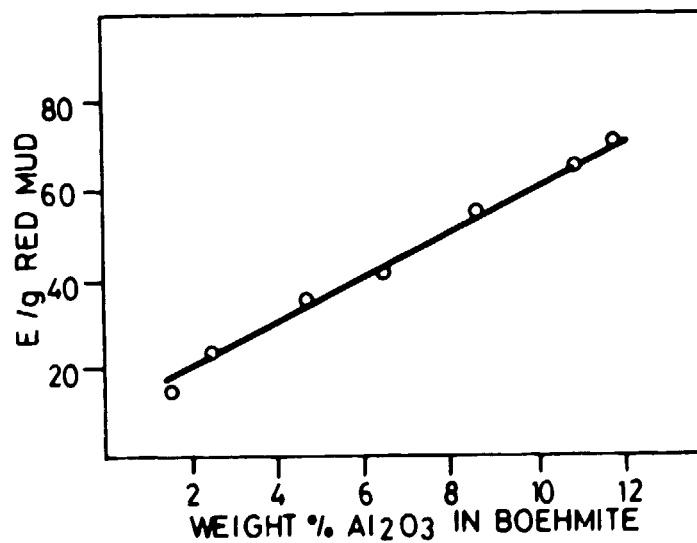


Fig. 4.39

CALIBRATION CURVE FOR THE DETERMINATION OF UNDISSOLVED BOEHMITE IN RED MUD BY THE 3100 cm<sup>-1</sup> INFRARED BAND

## IR SPECTROMETRY

It has been explained in respect of the quantitative IR phase analysis of bauxites that synthetic minerals or mixtures prepared from pure concretions cannot be used for the construction of calibration curves since the intensity (extinction coefficient) of the infrared bands of these may considerably differ from those of the minerals found in bauxite. Therefore the calibration must be accomplished with standard bauxite samples of known phase composition, originating from the same or similar area as the sample to be analysed.

Taking into account the above principles in the case of the analysis of red muds too, the calibration curves can be established on the basis of mixtures, containing red mud originating from the industrial processing of the relevant bauxite. The amount of the undissolved boehmite and that of the hydrargillite formed by hydrolysis in the red mud as well as the kaolinite content of the desilicated slurries is - in the case of normal operation - only a few percent. Thus from that point of view it is important to detect these minerals even in low concentrations, and it was proved that this is possible using IR spectrometry (Jónás, Solymár and Orbán, 1974).

The calibration curve for the determination of boehmite based on its O-H stretching vibration band at  $3100\text{ cm}^{-1}$  is shown in Fig.4.39.

The quantitative determination of kaolinite can be based on the  $3700\text{ cm}^{-1}$  O-H stretching band. The other characteristic band ( $917\text{ cm}^{-1}$ ), which is suitable for quantitative analysis in the case of bauxite, is now disturbed by the strong absorption of sodalite and cancrinite.

The quantitative determination of hydrargillite can be carried out on the basis of the  $3455\text{ cm}^{-1}$  or the  $3530\text{ cm}^{-1}$  O-H stretching band. The calibration curves can be constructed with the same mixtures as used for the boehmite calibration.

Cancrinite has three infrared bands which do not appear in the sodalite spectrum, namely the bands at 560, 625 and  $1105\text{ cm}^{-1}$ . The  $560\text{ cm}^{-1}$  band is not suitable for the analysis of cancrinite in red mud because it coincides with a strong hematite band. Calibration curves based on the 625 and  $1105\text{ cm}^{-1}$  bands, respectively are reproduced in Fig.4.40.

In the spectrum of pure synthetic sodalite (prepared in laboratory) there are two bands that do not overlap with the cancrinite bands ( $720$  and  $740\text{ cm}^{-1}$ ), thus in principle it is possible to determine also the sodalite by a direct IR method.

The infrared spectra of several industrial red mud samples have been studied and although this samples did contain sodalite the above mentioned two bands hardly appeared, if at all. It is very probable that sodalites of intermediate structures were present. Synthetic sodalites prepared in laboratory in the presence of various additives gave the  $720\text{ cm}^{-1}$  bands intensively only in the case of chloride sodalite.

During the Bayer process alumogothite gets into the red mud unchanged (unless special leaching conditions are applied). Consequently in the spectrum of red mud the maximum of goethite band around  $800\text{ cm}^{-1}$  appears shifted to  $820\text{-}830\text{ cm}^{-1}$  and its intensity seems to be very low. For this reason and because the intensity of this band depends strongly on the aluminium content of goethite, this band is not suitable for quantitative analysis. Nevertheless, the wave number at which the peak appears is characteristic for the aluminium content of the goethite, thus it gives information upon one of the factors of aluminium loss in the Bayer process.

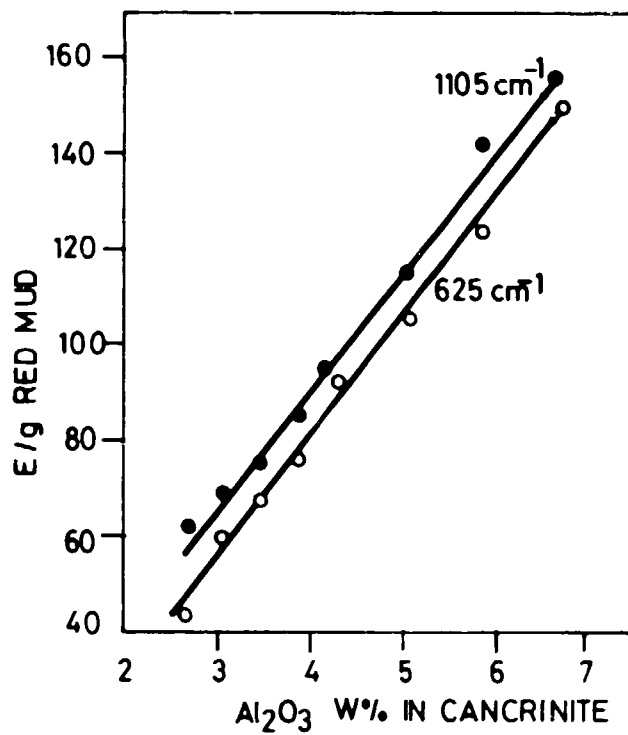


Fig. 4.40

CALIBRATION CURVES FOR THE DETERMINATION  
OF CANCRINITE IN RED MUD

## QUANTITATIVE PHASE ANALYSIS OF RED MUDS

The method of computer aided diffractometric quantitative analysis can also be used for red muds, however, it fails if serious uncertainties exist as regards the chemical composition of the crystalline components.

The final data should be fixed by the complementary use of X-ray diffractometry, IR spectrometry and thermal analysis. The particular merits of these methods were underlined in the corresponding sections.

The following limits of detection can be stated for the crystalline phases of red mud when the discussed methods are being applied:

Phase	Limit of detectability
Gibbsite	0.3 %
Boehmite	0.3 %
Sodalite	1 %
Cancrinite	1 %
Goethite	1 %
Hematite	0.5 %
Diaspore	0.5 %
Chamosite	1 %
Quartz	0.3 %
Calcium aluminate	1 %
Calcium titanate	0.5 %
Maghemite	1 %

#### 4. MINERALOGICAL INVESTIGATION OF ALUMINA

Although the alumina (being the end product of the Bayer process is not a natural mineral but a synthetic material gained by the calcination of aluminium trihydrate, it can be well characterized using some mineralogic techniques.

The main crystalline component of the Bayer alumina is normally corundum ( $\alpha\text{-Al}_2\text{O}_3$ ). The percentage and grain-size/shape of this depends upon the temperature of calcination and the additives, if any. Other constituents are sodium-beta-aluminate,  $\gamma\text{-Al}_2\text{O}_3$  and amorphous alumina.

##### OPTICAL METHODS

A very simple, inexpensive but rather time consuming method is based on microscopy. After staining alumina by methylen blue the corundum particles can be easily distinguished under the microscope. The alumina powder must be dispersed on a slide glass and a raster in the field of view aids the systematic evaluation of a large number of particles. A mechanical counting device can render the bookkeeping of the counts reliable and effective.

Scanning electronmicroscopic images, of course, can be analysed similarly. However, the corresponding sophisticated instrumentation costs several orders of magnitude more than a simple optical microscope and count register.

##### X-RAY DIFFRACTION METHODS

Referring to alumina studies the share of X-ray photographic techniques may be equally important as that of diffractometric measurements. This is due partly to the circumstance that alumina has very low iron content and, therefore, the use of a reflected beam monochromator is not

necessary. Another reason is that Guinier type photographs yield accurate powder data within a short time using very small samples.

Photometric evaluation of such films can lead to quantitative phase determination after appropriate calibration procedures.

However, measurement of corundum percentages can be accomplished faster by means of diffractometry. This is especially valid for "normal" alumina produced without additives and calcined at a temperature not higher than 900 °C. For this material the measurement of a single reflection seems to be sufficient. Using pulse counting procedure the integrated intensity under the peak is measured and corrected for the background scattering measured at both sides of the reflection.

The calibration of this intensity as a function of corundum content can be carried out using synthetic mixtures of known composition. For accurate measurements it is justified to control the counts obtained from standards embracing the compositional range represented by the unknown samples in each series of determinations. The error of the corundum percentage obtained in this way is lower than  $\pm 2\%$  and only a few minutes of time is needed per sample (the more samples are controlled in one cycle the less the share of an individual measurement).

When the alumina had been doped or calcined at elevated temperatures exceeding 900 °C difficulties appear concerning the effects of preferred orientation. Although several proposals have been put forward to remedy this situation, no perfect solution is known yet.

## REFERENCES

- Alexander L.E. (1976) Forty years of quantitative diffraction analysis, *Adv. X-ray Anal.* 20, 1-13.
- Bárdossy Gy. (1975) The complex methods developed in Hungary for the mineralogical-petrological and geochemical evaluation of bauxites, *VAMI-FKI - 2*, 27-42.
- Bárdossy Gy. (1979) *Karstic bauxites*, Hilger Publ. House, London.
- Bárdossy Gy., Csanády Á. and Csordás A. (1978) Scanning electron microscope study of bauxites of different ages and origins, *Clays and Clay Minerals* 26, 245-261.
- Bárdossy Gy., Jónás K., Imre A. and Solymár K. (1977) Interrelations of bauxite texture, micromorphology, mineral individualism and heteromorphism, *Economic Geol.* 72, 573-581.
- Bárdossy Gy., Vassel K.R. and Árkossy K. (1975) Quantitative phase analysis and texture of typical Hungarian and Soviet bauxite samples, *VAMI-FKI - 2*, 43-142.
- Bárdossy Gy. and Panthó Gy. (1973) Mineral and element investigation in bauxites by electron-probe, *ICSOBA 3<sup>e</sup> Cong.Int., Nice*, 47-53.
- Bárdossy Gy. and Panthó Gy. (1971) Investigation of bauxites with the help of electron probe, *Tschermaks Min.Petr. Mitt.Wien*, 15, 165-184.
- Bárdossy Gy., Bottyán L., Gadó P., Cziger Á. and Sasvári J. (1979) Computer based quantitative mineralogical phase analysis of bauxites *Amer. Miner* (in press.).



- Brown G.(ed) (1961) The X-ray identification and crystal structures of clay minerals, Mineralogical Society, London.
- Gadó P. and Orbán M. (1979) Automated quantitative mineralogical phase analysis of bauxites and red muds, AIME Annual Meeting, New Orleans, LM -
- Jenkins R. and Vries J.L.de (1970) An introduction to X-ray powder diffractometry, N.V.Philips Gloeilampenfabrieken, Eindhoven, Holland.
- Jónás K. and Solymár K. (1976) Study of the heteromorph nature of bauxite minerals by infrared differential spectroscopy Travaux ICSOBA 13, 391-400.
- Jónás K., Solymár K. and Orbán M. (1974) Phase analysis of red mud by infrared spectrometry, Acta Chim.Acad.Sci. Hung. 81, 443-453.
- Jónás K., Solymár K. and Orbán M. (1973) Phase analysis and characterisation of bauxites and red muds by infra-red spectrometry, ICSOBA 3<sup>e</sup> Cong.Int., Nice 325-330.
- Lahodny-Sanc O., Bokor B.F., Stanek J. and Hulinsky V. (1972) Electron microscope study of bauxites, Proc.Int.Clay Conf., 781-784.
- Mackenzie R.C. (1957) The differential thermal investigation of clays, Mineralogical Society, London.
- Orbán M., Imre A. and Stefániay V. (1976) Complex mineralogical investigation and characterization of bauxite and red mud, Travaux ICSOBA 13, 491-506.

Orbán-Kelemen M., Kotsis T. and Sajó-Feszl M. (1975)  
Quantitative phase analysis of red muds, VAMI-FKI  
267-294.

Sabiston G.H. (1975) Mineralogical applications in characteriz-  
ing raw materials and intermediate products of the alu-  
minium industry, J.Geol.Soc.Jamaica, Proc.of Bauxite  
Symposium, No.III, May 17, 44-56.

Solymár K. and Kenyeres-Süke S. (1966) Derivatographic  
determination of mineral composition of red muds, Proc.  
Anal.Chem.Conf., Budapest, 395-410.

White J.L. (1974) Evaluation of bauxites by infrared tech-  
niques Travaux d'ICSOBA 12, 25-31.

Zámbó J. and Solymár K. (1973) Prospects of phase transforma-  
tions in the Bayer process, ICSOBA 3<sup>e</sup> Cong.Int., Nice,  
491-502.

